A Mathematical Model of the Effects of Spatio-Temporal Patterns of Dendritic Input Potentials on Neuronal Somatic Membrane Potentials

by

George Morgan Barnwell
Biomathematics Program
Department of Statistics

Institute of Statistics Mimeo Series No. 750

TABLE OF CONTENTS

LIST OF TABLES

LIST OF FIGURES

LIST OF FIGURES (continued)

INTRODUCTION

The purpose of this thesis is to study certain aspects of neuronal function from a mathematical point of view, and, in particular, some aspects which may prove to be of special importance in the processes of learning and memory. A mathematical model of an idealized neuron will be developed and will serve as the basis of a computer simulation study of the integrative electrical properties of neurons.

Before constructing the particular model relevant to the problem, it is worthwhile to consider the value of mathematical models in neurophysiology, or any other area of biology. What does a mathematical model offer that could not be achieved by logical thinking and qualitative insights about a biological system? Can the model show something which was not already obvious, or at least deducible, from the body of experimental literature? Harmon's (1964, p. 15) opinion of the value of a model is stated:

> Any model has utility only insofar as it raises questions, suggests new relationships, and serves to focus one's thoughts. This is accomplished by using it to test hypotheses, to compute, to extrapolate and predict, and to suggest useful experiments. In this way models accelerate the process of learning about the real world.

Rall (1965) points out that mathematical models for computer simulation of complex systems can help an investigator decide whether a particularly complex and costly experiment is worth performing (by first simulating the experiment) and can contribute to the design of further experiments.

The role of mathematics in neurophysiology or in any other area of biology could thus be regarded as a methodology or a set of techniques

which allow the examination of relationships which would not always be apparent. Just as a microscope allows us to examine objects and relationships between objects which would not be seen otherwise, mathematics may be used to study complex interrelationships which are difficult to understand by other approaches. The general procedure in studying a complex system by mathematical modeling is to give precise definitions to the elements of the system, to specify certain simplifying assumptions, to construct the model and to examine the behavior of the model in order to make inferences about the system.

Some critics of mathematical models may point to the simplifying assumptions in a mathematical model as indicative that the model bears little resemblance to the real system. However, even in experimental biology, similar (many times implicit) assumptions are basic to methodology. For example, an object which is fixed, stained, sectioned, and mounted on slides may be quite different (e.g., in size and shape) from the object in the intact organism. Yet the structure of the intact object in the living organism is inferred from such studies. As Rall (1965, p. 239) further points out with reference to neurophysiology:

> ...any good experimental neurophysiologist can provide an extensive catalog of the unphysiological conditions of most experiments; the fact that we have come to accept the artificiality of such experiments does not do away with a fundamental uncertainty about the relation of the experimental preparation to the normal intact animal.

That mathematical models have already played an important role in neurophysiology is obvious when one examines the mathematical treatments

reviewed in the books by Cole (1968) and Plonsey (1969), for example. The extensive work of W. Rall (to be reviewed below) is further evidence of the contribution of mathematics to the area. Mathematical models developed for computer simulation studies will undoubtedly play an even greater role in the future blending of neurophysiological theory and experiment.

With the above arguments in mind, it is appropriate to state the goals of the present study. For potential changes of small amplitude, the theoretical effects of varying synaptic efficacies, varying synaptic temporal input patterns, and varying locations of synapses upon neuronal somatic membrane potentials will be studied.

Specific purposes of the study are to consider the effects of various combinations of the following factors upon somatic membrane potentials:

(a) A single excitatory synapse placed at different locations on a single dendritic branch,

(b) Different temporal input patterns arriving at a synapse (only deterministic patterns are considered in the present study, but stochastic patterns could also be employed),

(c) Different quantal amounts of transmitter released, where the amount of transmitter released per impulse may be either a stochastic or deterministic variable (only deterministic variables are considered here),

(d) Combinations of the above factors for more than one synapse and more than one dendritic branch.

Several theoretical questions may be at least partially answered by such an investigation, such as

(1) For a synapse of fixed efficacy at a fixed location on a neuron, is there some optimal temporal input pattern at this synapse which results in a maximum amount of depolarization at the soma?

(2) If there are optimal temporal input patterns as in question 1, would changes in the amount of transmitter released per impulse have any effect on the optimal pattern, and if so, how?

(3) What are the consequences of some hypothetical learning and memory mechanisms upon excitability of the neuron in the future?

(4) How do dendritic miniature postsynaptic potentials contribute to the experimentally recorded PSP profiles?

REVIEW OF LITERATURE

Many hypotheses concerning the physiological-biochemical bases of learning and memory have been advanced in recent years, e.g., Hyden (1959), Katz and Halstead (1950), Gaito (1961, 1963), Gaito and Zavala (1964), Griffith and Mahler (1969), Galambos (1961), Hebb (1949), and Briggs and Kitto (1962). Several of these hypotheses include little or no consideration of the properties of individual neurons, such as those which suggest that memory is encoded into nucleic acids by base sequence changes (Hyden, 1959; Gaito 1961, 1963). Others e.g., Hebb (1949) have postulated synaptic plasticity as the fundamental change involved in learning and memory, without sufficient consideration of the electrophysiological consequences of the postulated change upon the function of neurons. Numerous mathematical models of the behavior of assemblies of neurons or neural nets have also been proposed as partial mechanisms involved in brain functions, and particularly in learning and memory processes (e.g., see the review by Harmon and Lewis, 1966). Several neural net models have considered only spatial summation of excitation and inhibition in a neuron, and have idealized neurons as point summing capacitors or logical elements as McCulloch-Pitts neurons (e.g., McCulloch and Pitts 1943; von Neumann, 1956). It seems likely that the processes underlying learning and memory ultimately depend on the behavior of neurons, and that the complete resolution of input-output phenomena in the single neuron is a prerequisite to the understanding of any complex process involving interactions between neurons. By answering the questions

raised in the introduction, one could have at least some theoretical framework for considering possible types of interactions between neurons and possible consequences of several hypothesized physiological-biochemical changes in a neuron upon its excitability in the future. Perhaps it might even be possible to show that for low input frequencies restricted to axosomatic synapses, the McCulloch-Pitts neural elements are not a bad approximation to the behavior of real neurons. However, it is desirable to consider more complicated models of a single neuron before any decisions about such simplifying assumptions may be made. In particular, the McCulloch-Pitts type models have a major shortcoming in that they make no allowances for the existence of axodendritic synapses. Although many neurophysiologists had minimized the possible role of dendritic inputs in contributing to depolarization of the somatic membrane, recent work by Rall (1959, 1960, 1962, 1964) has shown that dendritic inputs play an important role in neuronal excitability.

Rall (1960) demonstrated theoretically that the then currently accepted estimates of motoneuron membrane time constants and resistivity, which did not give adequate weight to the relatively much larger area and conductance contributions of the dendrites as opposed to the soma, were too small. Rall's (1960) method yielded membrane time constant estimates about 75 per cent larger than methods which ignored dendritic contributions (Coombs, et al., 1959). Rall (1959) showed that underestimation of dendritic dimensions by Eccles and others (1957, 1959) led to significant underestimates of motoneuron

membrane resistance by a factor as large as ten (e.g., Rall's values were around 4700-7000 Ω cm^2, as opposed to previous estimates around 400-600 Ω cm^2).

As Rall (1962) points out, the reasons for underestimating the functional significance of dendrites were that the total surface areas of dendrites relative to the soma were not given adequate consideration, due to the prevailing opinions that excitatory dendritic inputs would decay so much in propagating to the soma that they would have negligible effects on somatic membrane potential, and that the density of dendritic synapses was thought to be much lower than that of somatic synapses. In a series of related papers, Rall (1959, 1960, 1962, 1964) has developed a mathematical model of a neuron which theoretically demonstrates the possible functional role of the dendrites. The consequences of Rall's model have been investigated by Rall and his associates in a series of studies utilizing computer simulation and experiments on cat spinal mononeurons (Rall, 1959, 1960, 1962, 1964, 1965, 1967, 1969a, 1969b; Smith et al., 1967; Nelson and Frank, 1967; Burke, 1967; Rall et al., 1967; Nelson and Lux, 1970). Detailed discussion of these and other experimental studies will be deferred until later. His model may be simply considered in three stages, as summarized by Rall (1964). He begins with an equivalent circuit which represents the electrical properties of a unit patch of nerve membrane, then shows that certain classes of dendritic trees are mathematically equivalent to cylinders so that the cable equation applies to potential changes along them, and finally explores various spatio-temporal input patterns with a compartmental

model, in which the soma and dendritic regions at different distances from the soma are treated as compartments.

Because Rall's compartmental model is not easily applicable to the questions posed in the introduction (see Rall, 1964, p. 86), an alternative approach is developed below. Spatio-temporal synaptic activation patterns composed of effectively non-interacting post-synaptic potentials (PSPs) of small amplitude are considered as inputs to a nonhomogeneous cable equation based on Rall's equivalent circuit and equivalent cylinder models. Such an approach allows consideration of the effects of various temporal input sequences which have not been explored with Rall's compartmental model. The assumptions inherent in Rall's models and the present model are discussed in detail in a subsequent section.

A few other mathematical models have been concerned with areas related to the questions in the introduction, with respect to the effects of synaptic input patterns upon somatic membrane potentials.

MacGregor (1966, 1967, 1968) considers various spatio-temporal input patterns in both somatic and dendritic regions and uses a computer model to calculate the resulting theoretical firing frequencies of neurons. However, the underlying mathematical foundations and accompanying assumptions are not clearly developed.

Sabah and Leibovic (1969) considered subthreshhold oscillatory behavior of the classical cable model by allowing membrane conductance to be voltage-dependent as in the Hodgkin-Huxley model. Calculations were made for various voltage step, current step, and current pulse inputs. Successive temporal inputs were not considered.

Swigert (1970) presents a mode control model which outlines conditions for three different modes of signal propagation in dendrites--a wave equation mode, a diffusion mode, and a pulse mode. Swigert concludes that in the diffusion mode (which corresponds to electrotonic spread as described by the cable equation) the transport of a signal in the dendrites is blocked, while in either the pulse or wave mode the transport of a signal down the membrane could be effected. At face value, such a conclusion would seem to imply that the pulse or wave modes are more effective means for propagation of signals in dendrites, and raise questions as to the applicability of the cable equation to dendrites. However, if the neuron is to possess any integrative functions, it seems desirable for dendrites to operate in a diffusion mode, so that signals are damped. Otherwise, if the dendrites always operated in wave or pulse modes, every incoming signal could be transmitted to the soma at full strength and there would be no need for integrative properties. By operating in the diffusion mode, the dendrites would filter out single signals, so that only higher frequencies of inputs at a single synapse, many simultaneous inputs at several synapses, or sustained levels of spatio-temporally scattered dendritic inputs are sufficiently integrated to produce effective potential changes at the soma.

Hartline and Cooke (1969) used a mathematical model to predict the form of postsynaptic membrane responses from various presynaptic input patterns in the lobster cardiac ganglion. The form of their equation resembles the input potential transients expressed as the right-hand-side of equation (11) in the present model. However,

Hartline and Cooke considered the membrane potential as a function only of time and not of distance of the synapse from the soma. Their theoretical postsynaptic response predicted from their model showed good agreement with actual recorded responses in some cases, but poor fits in others.

THEORY

In order to investigate the questions raised in the Introduction, a mathematical model of the effects of various combinations of spatio-temporal synaptic activations consisting of small amplitude potential transients, upon somatic membrane potential in a single neuron will be developed. It should then be possible to examine the theoretical consequences of changing various parameters in the model, in terms of excitability of the neuron. The model to be developed below depends upon several of the assumptions of the equivalent circuit model, of cable theory, and of Rall's equivalent cylinder model. Each of these models will be first discussed with respect to their underlying assumptions, and then the present model will be developed.

Equivalent circuit

The electrical behavior of a unit area of membrane is represented by the equivalent circuit [1] of Figure 1(a). The particular model shown uses Rall's more general notation, but is related to those of Fatt and Katz (1953), Coombs et al., (1955b), and Hodgkin and Huxley (1952). The model consists of four parallel pathways for current flow through the membrane. The membrane capacity per unit area is denoted by C_m. The membrane conductances per unit area are G_r, G_ε, and G_j, where the subscripts r, ε, and j designate pathways respectively associated with the resting membrane, excitation, and inhibition. The membrane resistances are $R_m = 1/G_r$, $R_\varepsilon = 1/G_\varepsilon$, and $R_j = 1/G_j$.

---

[1] The circuit is equivalent to the region of nerve membrane it represents in the sense that both have the same response to an applied current (Ruch et al., 1961, p. 48).

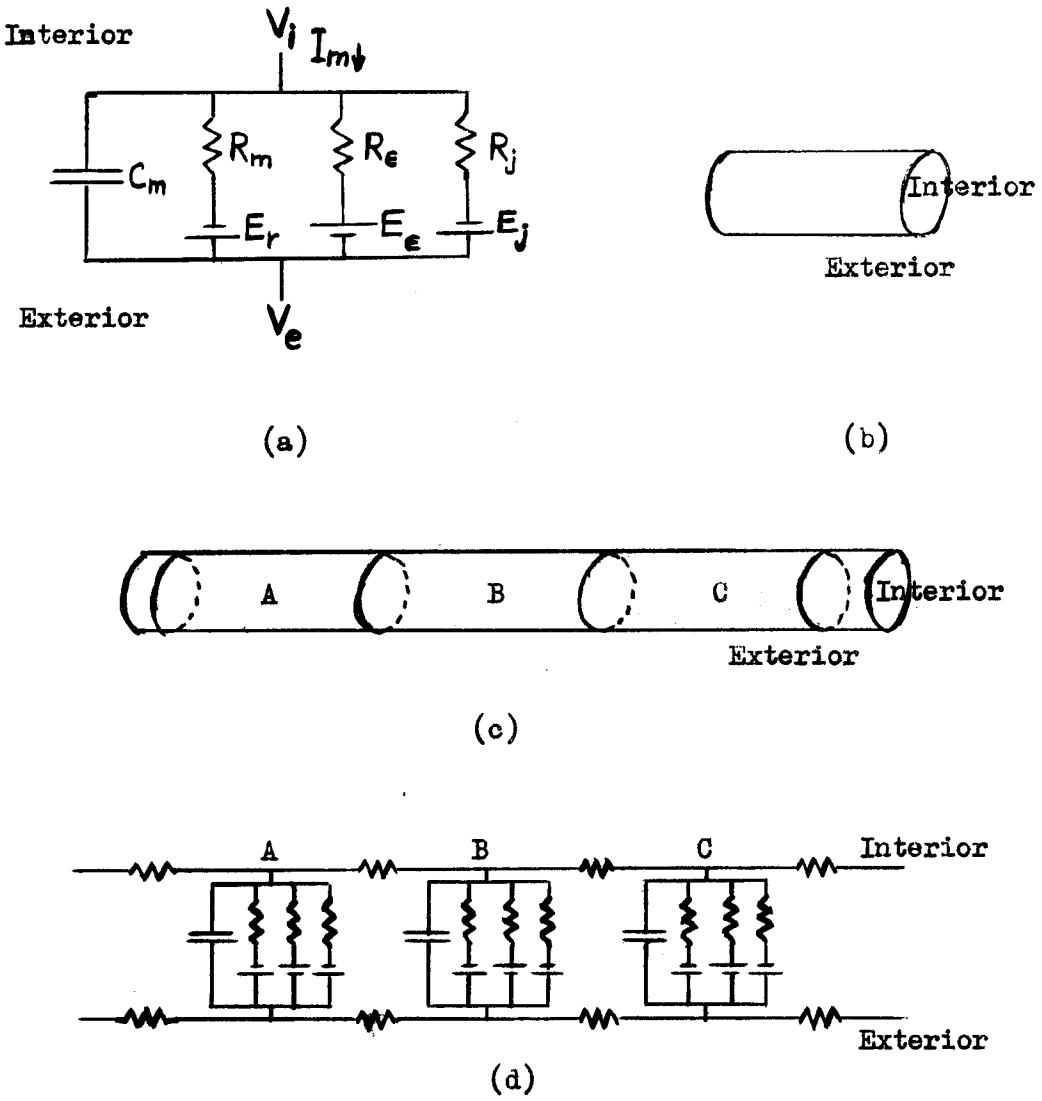

Figure 1. Relations between equivalent circuit model and cable theory.

(a) Equivalent circuit representation of electrical behavior of a unit area of membrane. See text for discussion.

(b) Cylindrical membrane element of unit area, which is represented by equivalent circuit of Figure 1(a).

(c) Three elements of unit area in cylinder are labeled A, B, and C, corresponding to the respective equivalent circuit elements in Figure 1(d).

(d) Labeled elements A, B, and C correspond to those of Figure 1(c), showing how connections between successive elements are represented by longitudinal resistances between them.

The equilibrium potentials or batteries for the respective pathways are E_r, E_ε, and E_j. The external conducting medium is at potential V_e, and the internal conducting medium is at potential V_i. The membrane potential V_m is defined as $V_m = V_i - V_e$. The total current flow through the membrane I_m, is simply the sum of the currents through each of the parallel pathways. The capacitative current is given by $C_m \frac{dV}{dt}_m$. The three ionic currents are $I_r = G_r (V_m - E_r)$, $I_\varepsilon = G_\varepsilon(V_m - E_\varepsilon)$, and $I_j = G_j(V_m - E_j)$. Thus, the total membrane current is given by

$$(1) \quad I_m = C_m \frac{dV}{dt}_m + G_r(V_m - E_r) + G_\varepsilon(V_m - E_\varepsilon) + G_j(V_m - E_j).$$

Evidence that the capacitative and ionic currents are in parallel is given by Hodgkin and Huxley (1952, p. 505). The values of E_r, E_ε, E_j, C_m, and G_r are assumed constant in Rall's model. These parameters were also assumed to remain constant by Hodgkin and Huxley (1952, p. 500) on the basis of their experimental results. Rall (1964) also assumed G_ε and G_j to be independent of membrane potential, since his model dealt with dendritic membranes, which are supposed to be chemically excitable, in contrast to the voltage dependence of the corresponding conductances g_{Na} and g_K in the Hodgkin-Huxley model, which dealt with axonal electrically excitable membranes.

The distinction between chemically vs. electrically excitable membranes is primarily one of positive feedback (Grundfest, 1967). In a chemically excitable membrane, conductance changes are produced by action of a chemical transmitter, and these conductance changes in turn

produce voltage changes. The conductance is independent of voltage, so that the induced voltage changes do not induce further conductance changes. In electrically excitable membranes, conductance changes are produced by voltage changes, and these conductance changes may in turn produce further voltage changes, so conductances are voltage dependent.

A summary of the assumptions in the equivalent circuit model is below:

1. There are four parallel pathways for current through the membrane, one capacitative and three ionic.

2. The values of E_r, E_ε, E_j, C_m and G_r are assumed to be constant.

3. The conductances G_ε and G_j are assumed to be independent of membrane potential by Rall, while the corresponding conductances g_{Na} and g_K are assumed to be dependent on membrane voltage by Hodgkin and Huxley.

Cable Theory

The cable equation describes the passive spread of potential in a nerve fiber. When the fiber is at rest, the internal and external voltages, and thus the membrane voltage, are constant and uniform over the length of the fiber. If the potential is changed at some point on the fiber, the cable equation describes the spread of this potential change. The potential change is defined as $V = V_m - E_r$, where V is a function of both the distance along the fiber, x, and time, t, i.e., $V = V(x,t)$. The cable equation in homogeneous form is

$$(2) \quad \lambda^2 \frac{\partial^2 V(x,t)}{\partial x^2} - \tau \frac{\partial V(x,t)}{\partial t} - V(x,t) = 0.$$

The terms τ and λ are respectively the membrane time constant and the characteristic length. The membrane time constant is defined as $\tau = R_m C_m$, in terms of the equivalent circuit membrane resistance and capacitance. The characteristic length is defined

$$\lambda = \left[\left(\frac{R_m}{R_i}\right)\left(\frac{r}{2}\right)\right]^{\frac{1}{2}} ,$$

where R_i is the specific resistance of the intracellular medium, and r is the radius of the nerve fiber, and where it is assumed that the extracellular resistance $R_e = 0$.

The relation between the equivalent circuit element and cable theory is shown in Figure 1. The equivalent circuit of Figure 1(a) may be considered to represent a ring of unit area as shown in Figure 1(b). When several such rings are linked together in a nerve fiber as in Figure 1(c), the longitudinal resistances between them may be added so that the whole fiber has the electrical representation of Figure 1(d).

The complete derivation of the cable equation may be found in several sources, e.g., Davis and Lorente de No, (1947), Cole (1968), and Hodgkin and Rushton (1946), and will not be repeated here. However, the underlying assumptions are also fundamental to the present model. The assumptions are concisely summarized by Hodgkin and Rushton (1946, p. 447):

> (1) The axon has a uniform cable-like structure with a conducting core, an external conducting path and a surface membrane with resistance and capacity.
> (2) The axon is sufficiently thin and the membrane resistance sufficiently high for the flow of current in core and interstitial fluid to be strictly parallel. An alternative statement of this assumption is that at any

given distance along the nerve the potential is constant throughout the core or throughout the external fluid.
(3) The axoplasm and external fluid behave as pure ohmic resistances.
(4) The membrane resistance is constant when the current density through the membrane is small.
(5) The membrane capacity behaves like a pure dielectric with no loss.

These are general assumptions which allow the differential equations for current or potential to be written. Each assumption is really an approximation, but we shall show later that no very serious errors are likely to result from their use. Certain experimental conditions must also be defined in order to allow the differential equations to be solved. These may be stated in the following way:
(1) The extrapolar and interpolar lengths are sufficiently long to be taken as infinite.
(2) The electrodes are sufficiently fine to be considered of zero breadth.
(3) A current of rectangular wave form is passed through the nerve.

Thus the derivation of standard cable theory is based on very long axons of small diameter, so that the potential change is considered to vary only in one spatial coordinate. On the basis of these assumptions, the applicability of the cable equation to dendrites of varying diameters and finite lengths should be carefully considered. Rall (1969) considered the distribution of membrane potential in cylindrical coordinates for cylinders of finite lengths and sealed ends, and derived formulas for calculating the errors obtained from the use of one-dimensional cable theory as opposed to the three-dimensional cable theory. He has shown that for cylinders whose diameters are small in comparison to their lengths, there is close agreement between one-dimensional cable theory and the more general formulation.

Dendritic trees and equivalent cylinders

Rall (1959) developed a mathematical model of the spread of current from a neuron soma into branching dendritic trees, based on cable theory. The assumptions essential to the model are, in slightly abridged form:

(1) A dendritic tree consists of a cylindrical trunk and cylindrical branch elements.

(2) The electric properties of the membrane are uniform over the entire soma-dendritic surface.

(3) The electric potential is constant over the entire external surface of the neuron. This is equivalent to infinite conductivity or zero resistivity of the external medium.

(4) The electric potential is constant over the internal surface of the some membrane. With regard to this assumption, Rall (1959, p. 494) states:

> Together with assumption 3, this implies a uniform soma membrane potential. In this formal model, therefore, the shape of the soma surface is irrelevant, because the entire soma membrane is effectively a lumped membrane impedance. Thus lumped impedance represents the common point of origin for all dendritic trunks belonging to a single neuron.

(5) The internal potential and current are continuous at all dendritic branch points and at the soma-dendritic junction.

(6) The current inside any cylinder flows axially through an ohmic resistance which is inversely proportional to the cross-sectional area.

(7) The current across the membrane is normal to the membrane surface. The uniformly distributed membrane impedance consists of an ohmic resistance in parallel with a perfect capacity.

(8) A membrane electromotive force, E, is in series with the membrane resistance, and is constant for all of the membrane. Under steady conditions, with no current flow, the electric potential difference, V_m, across the membrane is equal to E.

Rall (1962) extends and simplifies his model by considering a class of dendritic trees which is mathematically equivalent to a single unbranched cylinder. The derivation of these results will not be repeated here, but the essential definitions, assumptions, and certain equations will be enumerated. Rall begins with the classical cable equation, equation (2), and notes that it may be written as

$$(3) \quad \frac{\partial^2 V}{\partial X^2} - \frac{\partial V}{\partial T} - V = 0,$$

where $T = t/\tau$ is a normalized expression for time in terms of the membrane time constant, and $X = x/\lambda$ is a normalized expression of distance along the cylinder in terms of its characteristic length, λ.

Rall considers a dendritic tree defined by the number, n, of branches of equal radius present at any distance, x, from the soma, and the radius of the branches. Taper of dendritic branches may also be included in the model, but the theoretical calculations in both Rall's and the current study assume that the dendritic tree is composed entirely of cylindrical branch elements. In this case, Rall shows that

$$(4) \quad \frac{dZ}{dx} = \frac{1}{\lambda}$$

holds, where Z is the electrotonic distance from the soma. Rall states that Z may be considered a generalization of the variable $X = x/\lambda$, so that λ is allowed to vary.

The essential mathematical constraint in the transformation is that the sum of the diameters of the daughter branches each raised to the 3/2 power must be equal to the diameter of the parent branch to the 3/2 power. Finally, the cable equation for an equivalent cylinder is

$$(5) \quad \frac{\partial^2 V}{\partial Z^2} - \frac{\partial V}{\partial T} - V = 0.$$

The transformation from x to Z essentially transforms a dendritic tree of this class into an equivalent cylinder. Rall points out that a property of such a class of dendritic trees is that a constant increment ΔZ corresponds to a constant increment ΔA of surface area. The above equations imply two additional properties of the model which were not listed as assumptions in Rall's (1959) paper, but were termed assumptions by Rall in a later treatment (1964, p. 84). The first of these assumptions is that all terminal dendritic branches end with the same Z-value. The second is that spatiotemporal inputs must be uniform in all branches of a dendritic tree corresponding to a given Z-value. These two assumptions were regarded by Rall as limitations of the equivalent cylinder model. Rall (1964) extends his mathematical study of the functional significance of dendritic trees by introducing a compartmental model. Using the compartmental model, Rall (1964, 1965, 1967) has explored the effects of various spatio-temporal input

patterns on somatic membrane potential, but has not considered cases where repeated inputs occur at a single synapse. It is here that the present model diverges from that of Rall.

Present Theory

Since the distribution of electric potential along a cylindrical dendritic branch is assumed to be adequately described by the cable equation, it is of interest to consider the possibility of studying various spatio-temporal synaptic activation patterns as input functions in a nonhomogeneous cable equation. Such an approach allows the effects of complex temporal input patterns to be studied in the same framework as less complicated patterns (see equation 12). The consideration of only synaptic activations of small amplitude permits the reduction of the homogeneous, time-variant cable equation to a nonhomogeneous, time-invariant form with the input or driving function representing various spatio-temporal synaptic activation patterns, as shown below.

The previous sections outlined the relations between the equivalent circuit and cable theory. More explicit mathematical formulations make these relations more evident, and serve as a starting point for the more general approach of the present model.

From cable theory, the longitudinal current I_ℓ in a nerve fiber is

$$(6) \quad I_\ell = \frac{1}{r_i} \frac{\partial Vm}{\partial x} ,$$

where r_i is the axoplasmic or internal resistance per unit length, and the external specific resistance R_e (and hence r_e) is usually assumed

to be zero (Rall, 1959), so that the total longitudinal resistance per unit length is r_i. The current flowing through the membrane, I_m, is the change in the longitudinal current with distance along the fiber, i.e.,

$$(7) \quad I_m = \frac{\partial I_\ell}{\partial x} = \frac{1}{r_i} \frac{\partial^2 Vm}{\partial x^2} \quad .$$

Combining equations (1) and (7), and transposing terms yields

$$(8) \quad \frac{1}{r_i} \frac{\partial^2 Vm}{\partial x^2} - Cm \frac{\partial Vm}{\partial t} - G_r(V_m - E_r) - G_\varepsilon(V_m - E_\varepsilon) - G_j(V_m - E_j) = 0.$$

Equation (8) is a linear, homogeneous, time-variant equation, since the excitatory and inhibitory conductance terms may be of the form $G = G(x,t)$. An equation of this form is difficult to solve except for very simple cases. In order to handle more complex situations, it is desirable to have an equation of the form

$$(9) \quad a \frac{\partial^2 V}{\partial x^2}(x,t) - b \frac{\partial V}{\partial t}(x,t) - cV(x,t) = F(x,t),$$

where a, b, and c are constants, and $F(x,t)$ is an input forcing function whose components are voltage transients only. This equation is the nonhomogeneous, time-invariant form mentioned above. The reduction from the homogeneous, time-varient form to the nonhomogeneous, time-invariant form is effected by making certain simplifying assumptions and noting some relations which follow from previous discussion.

From the equivalent circuit model, $V_m = V + E_r$, so that this term may be substituted for V_m in equation (8). Since E_r was assumed

to be constant, it follows that

$$\frac{\partial^2 V_m}{\partial x^2} = \frac{\partial^2 V}{\partial x^2} \text{ and } \frac{\partial V_m}{\partial t} = \frac{\partial V}{\partial t} .$$

The present model will deal only with excitatory inputs, so that G_j is assumed to remain constant and is taken to be zero. Further, $G_r = 1/R_m$ was assumed to be constant in the equivalent circuit model. The remaining term, $G_\varepsilon(V + E_r - E_\varepsilon)$, involves excitatory conductances, and is time-variant. For excitatory conductance changes of sufficiently small amplitude, the amplitudes of the resulting voltage transients will also be small. Since the driving potential is defined as the difference $E_\varepsilon - V$, it may be assumed to remain constant for small V, i.e., $E_\varepsilon - V \sim E_\varepsilon$. Then the time-variance in the remaining term may be considered to be due to $G_\varepsilon = G_\varepsilon(x,t)$, and transposing this term to the right hand side of equation (8), making the above substitutions, and multiplying through by R_m yields

$$(10) \quad \frac{R_m}{r_i}\frac{\partial^2 V}{\partial x^2} - T\frac{\partial V}{\partial t} - V = R_m G_\varepsilon (E_r - E_\varepsilon),$$

a relationship in the potential V in which the right hand side is an input potential transient expression which is proportional to the excitatory conductance.

The arrival of excitatory transmitter at the post-synaptic membrane produces a change in the excitatory conductance, which allows ionic currents to flow through the membrane, and results in a corresponding voltage change. Since the amplitude of the resulting voltage transient is proportional to the quantal amount of transmitter released

(Martin, 1966; Katz, 1966), the voltage transient itself may be considered as the input function. Thus, under the conditions specified in the assumptions, the term involving $G_\varepsilon = G_\varepsilon(x,t)$ in equation (10) may be replaced by input terms involving voltage transients, as in equation (9). The model rests on several of the assumptions from the equivalent circuit, cable, and equivalent cylinder models. In particular, the first two assumptions and Rall's version of the third assumption of the equivalent cylinder model (see page 13), all eight of Rall's assumptions for the branching model of dendritic trees (see page 16), in addition to the specifications for the equivalent cylinder model (see pages 17-19) are applicable. The Hodgkin-Rushton assumptions for the cable model which apply to the present model are included in the list of Rall's assumptions. Additional assumptions inherent in the present model are presented below:

It is assumed that:

(1) The spread of electrotonic potential in a cylindrical dendritic branch or an equivalent cylinder is described by the cable equation. This assumption has been discussed in previous sections, and no further comments are necessary, aside from stating that there is no known evidence which contraindicates the applicability of the cable equation to dendrites and equivalent cylinders.

(2) The activation at either an excitatory or inhibitory synaptic site is produced by a chemical transmitter which is released in quantal packets. This assumption is supported by a great deal of physiological evidence (e.g., see reviews by Martin, 1966, Katz, 1966 and Eccles, 1964).

The present model is not concerned with electrically transmitting synapses.

(3) The response to a single quantum of transmitter at the post-synaptic membrane is a potential change, which for the membrane initially at rest, is always of the same form, and has the same magnitude and time course. This response will be termed the unit post-synaptic potential (unit PSP), with the adjectives "excitatory" or "inhibitory" added to denote the type of synapse when it is not obvious from the eontext. The shape of the unit PSP is given some mathematically convenient form which fits empirical curves. This assumption treats the response of the post-synaptic membrane to a single quantal packet of transmitter as a potential change. In reality, the primary effect of transmitter substance is to produce a conductance change in the post-synaptic membrane, which results in a movement of ions through the membrane and a corresponding voltage transient, as mentioned above. The assumption that the driving potential is effectively constant for small PSPs leads to the present assumption.

(4) The potential change of the post-synaptic membrane for a given pre-synaptic impulse is representable as a linear combination of unit PSPs, each weighted in a manner proportional to the number of quantal units of transmitter released. This assumption is valid for small PSPs. Nonlinear summation of PSPs has been reported for large amplitudes (Martin, 1966).

(5) The maximum amplitude of potential changes in the post-synaptic membrane produced by summation of unit PSPs is restricted to about 5% of the driving potential of the resting membrane. For a driving

potential of 80 mV magnitude, this maximum value would be 4 mV. This is the assumption made in converting the linear, time-variant, homogeneous cable equation to the time-invariant, nonhomogeneous form, so that the approximation of constant driving potential is essentially the approximation $E_\varepsilon - V \approx E_\varepsilon$.

(6) The number of quanta of transmitter released for a particular impulse may be distributed according to a Poisson distribution, or may be considered a deterministic variable. There is a considerable amount of evidence in support of the first part of this assumption (see reviews by Martin, 1966, and Katz, 1966). The assumption that the amount of transmitter released per impulse may be a deterministic variable is made in order to facilitate consideration of the theoretical effects of certain learning and memory mechanisms, and of relations between rates of release, synthesis, and storage of transmitter in the presynaptic terminal.

(7) The particular activation times for each synaptic site may be determined either stochastically or deterministically (e.g., a fixed frequency), so that the theoretical effects of any desired form of temporal input sequence at any synaptic site may be studied.

(8) The synaptic activations provide the input or driving mechanism for the potential changes which are propagated along the dendrites. Assumption 8 is related to assumption 3 in the sense that the potential change is assumed to be the driving mechanism, rather than the conductance change. Since a potential change at one point of a nerve fiber does induce potential changes at neighboring points, and thus spreads along the fiber, the assumption that input potential transients serve as a driving mechanism seems valid.

(9) The width or diameter of any synaptic region, with respect to the length along the cylinder, is assumed to be zero. Thus, each synapse along a cylinder is treated as a point and a delta function may be used to specify the locations of these points. This assumption is rather artificial, since the synapses have finite widths, and is made strictly for purposes of mathematical simplification. However, since the widths of synapses are small, the treatment of electrotonic distance of a synapse from the end of the cylinder to the center of the synapse would result in a spatial error of at most d/2, where d is the synaptic diameter. For example, an assumed synaptic diameter of 1 μ falls within the range of experimentally observed diameters of synaptic end bulbs in a cat spinal cord (Haggar and Barr, 1950; Illis, 1964). The spatial error in this case would be only 0.5 μ.

(10) The neuron is first mathematically idealized as essentially a pair of branched dendritic trees whose junction is the soma and whose remote branches are at an infinite distance from the soma. Then the further idealization resulting from the use of the equivalent cylinder model is a cylindrical neuron of infinite length, whose soma is centered at the origin. Thus the Z-axis goes from $-\infty$ to $+\infty$. Inputs are considered to occur in the positive half of the Z-axis, so that the negative half may be regarded as another dendritic trunk into which potential may spread after passing the soma. The counterbalancing of each incoming equivalent cylinder by its identical negative counterpart is a mathematical assumption which permits the use of equations (16) through (19), and such perfect symmetry is not likely to be seen in an actual neuron. The axon is also neglected, but since the interest of

the present model is only in the somatic potential and not in what propagates past the soma, these approximations seem reasonable for a preliminary model. Further, for dendritic trees whose peripheral branches are 5 or more characteristic lengths from the soma, the dendritic tree may be regarded as essentially infinite in length. With these assumptions, the general form of the input forcing function (now in terms of the variable Z instead of x) in equation (9) may be expressed as

$$(11)\quad F(Z,T) = \sum_{j=1}^{m} \sum_{k=1}^{n_j} q_{jk}\, V_j(T,\, T_{jk})\, \delta(Z-Z_j),$$

for $Z_j \geq 0$, $0 \leq T_{jk} \leq T$, where $Z = 0$ denotes location of the soma, Z_j is the location of the jth synaptic site, T_{jk} is the kth activation time for the jth synapse, q_{jk} is the number of quantal releases for the jth site at time T_{jk}, $V_j(T, T_{jk})$ is the unit PSP at time T at the jth site due to activation at time T_{jk}, m = number of synapses, n_j = number of activations at jth synapse, for $T_{jk} \leq T$.

Equations (5) and (11) are combined in equation (12), which is the general statement of the model,

$$(12)\quad \frac{\partial^2 V}{\partial Z^2}(Z,T) - \frac{\partial V}{\partial T}(Z,T) - V(Z,T) = \sum_{j=1}^{m} \sum_{k=1}^{n_j} q_{jk} V_j(T,T_{jk})\delta(Z-Z_j),$$

for $Z_j \geq 0$, $0 \leq T_{jk} \leq T$, with the initial condition $V(Z,0) = \phi(Z) = 0$ for all real Z. Thus, equation (12) expresses the propagation of an electrical disturbance through a cylinder which is stimulated according to the spatio-temporal input pattern defined by the right-hand side. The effects of various deterministic or stochastic temporal input patterns at any number of synapses at various sites and for different

quantal amounts of transmitter released per impulse upon neuronal somatic membrane potential may thus be studied by changing the right-hand side of equation (12). The unit or miniature PSP expressed by $V_j\ (T,\ T_{jk})$ may have any form which fits experimentally obtained graphs. The particular form studied in the present model is

$$(13)\quad V_j(T,T_{jk}) = \left.\begin{array}{ll} [eA(T-T_{jk})/T_p]e^{-(T-T_{jk})/T_p}, & T-T_{jk} \leq T^* \\ = 0, & T-T_{jk} > T^* \end{array}\right\} \forall_j ,$$

where A is the maximum amplitude or peak value of the unit PSP, and T_p denotes the time to peak. The restriction on $V_j\ (T,\ T_{jk})$ with respect to the time interval T* provides a compact support for the input function in equation (12) which is sufficient to guarantee the existence of its solution. In the computer program, T* is the time it takes for the value of $V_j\ (T,\ T_{jk})$ to drop below 10^{-75}, after which it is set to zero. In equation (12), each unit PSP is represented by a term $V_j\ (T,\ T_{jk})$ which is multiplied by a term q_{jk} corresponding to the quantal amount of transmitter released for a given impulse at a given synapse.

Although the form of equation (12) would allow the effects of both excitatory and inhibitory inputs to be represented, only excitatory synapses are considered in the present computational model. The resting potential is much closer to the inhibitory equilibrium potential than to the excitatory equilibrium potential, so that the driving potential for an inhibitory synapse is much smaller. The small inhibitory driving potential means that the same type of approximation made for excitatory synapses cannot be made for inhibitory synapses,

i.e., one cannot safely say $E_j - V \approx E_j$, since even a small value of V could be as large in magnitude as E_j.

Under the assumption of linear summation of electrotonic potentials from separate dendritic trees arriving at the soma, the variables V and Z may be treated as vectors. The potential at any point Z on the ith equivalent cylinder at time T may be expressed as $V_i (Z_j, T)$, where Z_j is the electrotonic distance from the soma of the particular point on the ith cylinder. The potential at the soma is the sum given by

$$(14) \quad V_s(T) = \sum_{i=1}^{p} V_i(0,T),$$

where p is the number of cylinders.

Solution of nonhomogeneous equation

The homogeneous cable equation (5) is a second order, linear partial differential equation of parabolic type, and obtaining its solution constitutes a Cauchy problem. The Cauchy problem for equation (5) is to find a function V (Z, T) which is continuous at every point in the region $-\infty < Z < \infty$ and $T \geq 0$, which is bounded in Z and T, which satisfies equation (5), and which assumes values for T = 0 as specified by $V(Z, 0) = \phi(Z) = 0$. In particular, the solution to equation (9) for an impulse input and for zero initial conditions is called the fundamental solution or Green's function (Mackie, 1965). Thus equation (15) with the initial and boundary conditions as specified constitutes the system to be solved, and the corresponding Green's function is denoted $G(Z, \xi ; T, \tau)$.

$$(15)\quad \frac{\partial^2 V}{\partial Z^2} - \frac{\partial V}{\partial T} - V = \delta(Z-\xi)\delta(T-\tau),$$

for $-\infty < Z < \infty$, $T > 0$, $V(Z,0) = \phi(Z) = 0$.

The solution to equation (15) may be obtained by the method of Laplace or Fourier transforms. Once the fundamental solution $G(Z, \xi ; T, \tau)$ is known, the solution $V(Z, T)$ to the nonhomogeneous equation for any input function, say $H(Z, T)$ may be found by means of the relation expressed by

$$(16)\quad V(Z, T) = \int_0^T \int_{-\infty}^{\infty} G(Z, \xi ; T, \tau)\, H(\xi, \tau)\, d\xi\, d\tau,$$

including cases where $H(Z, T)$ is a generalized function or sum of generalized functions, if the components have compact support (Shilov, 1968). The fundamental solution to equation (15) is

$$(17)\quad G(Z, \xi ; T, \tau) = \frac{1}{2\sqrt{\pi}\sqrt{T-\tau}}\, e^{-(T-\tau)-\frac{(Z-\xi)^2}{4(T-\tau)}}$$

and the input function of interest is given above by equation (11), so that the solution of interest is

$$(18)\quad V(Z,T) = \int_0^T \int_{-\infty}^{\infty} G(Z, \xi ; T,\tau) \sum_{j=1}^{m} \sum_{k=1}^{n_j} q_{jk} V_j(T, T_{jk})\, \delta(\xi - Z_j)\, d\xi\, d\tau,$$

or,

$$(19)\quad V(Z,T) = \sum_{j=1}^{m} \int_0^T \frac{1}{2\sqrt{\pi}\sqrt{T-\tau}}\, e^{-(T-\tau)-\frac{(Z-Z_j)^2}{4(T-\tau)}} \sum_{k=1}^{n_j} q_{jk} V_j(\tau, T_{jk})\, d\tau.$$

The existence of such solutions involving generalized functions in the nonhomogeneous term has been established by Shilov (1968, chap. 3).

The general solution of the nonhomogeneous equation (12) is thus seen to be a sum of convolution integrals. This shows the electrotonic potential at any point along the cylinder at any time, resulting from a particular spatio-temporal input pattern.

Computer Model

The computer model consists of two main programs, a "bookkeeping" program which is used for complex deterministic spatio-temporal activation patterns or for stochastic patterns, and a computational program, which calculates the solutions for the various input combinations. Both programs are written in Fortran language for the IBM 360 system.

The bookkeeping program consists of subroutines which generate the desired stochastic or deterministic spatio-temporal activation patterns.

The computational program consists of subroutines which compute local dendritic potentials and somatic potentials as functions of the activation patterns, and then display them in digital plots. The computations involve finding a solution of equation (19) at the soma (i.e., at $Z = 0$) for any given spatio-temporal activation pattern occurring on the corresponding cylinder. If more than one cylinder is involved, equation (14) is the basis of computing integrated contributions from several cylinders.

RESULTS AND DISCUSSION

The effects of a variety of spatio-temporal input patterns were investigated, and quantitative comparisons of many types were made. The first computations were concerned with establishing reference values of the relative effects of changes in T_p, A, q, or Z upon dendritic and somatic potentials. Further computations explored effects of both simple and complex temporal activation patterns in a single cylindrical element. Then combined effects of complex temporal activation patterns in more than one cylindrical element were considered. The results of these calculations are divided into sections corresponding to the above topics, with additional sections concerning extra peaks, evidence from experimental neurophysiology, and implications for some hypothetical learning and memory mechanisms.

Effects of input parameters upon local and somatic PSPs

Initial computations were carried out to systematically explore the effects of changing the input parameters T_p, A, and q (the time-to-peak, peak amplitude, and quantal multiplier of the input potential transient), upon both the local dendritic potential and the somatic potential. For these calculations, a single activation at a single synaptic site constituted the input in each case.

As expected from the nature of the input potential transient function, increasing the value of the unit input amplitude parameter A, or the quantal multiplier q resulted in a proportional increase of the peak value of the local PSP and of the somatic potential. Figure 2 shows the effect of various values of q upon the local PSP, with

constant values of $T_p = 0.2$ and $A = 0.5$. Since A and q are both multipliers, the effects of either parameter may be seen by changing only one, so only q was changed for these calculations. Note that the time courses of the four curves were the same, and all peaks occurred at the same time, since T_p remained constant. The linear increase in PSP peak amplitude as a function of A or q is also obvious from the figure. For example, increasing the value of q from 2 to 4 also doubled the peak value of the PSP. An extensive listing of such relations between A or q and the PSP peak amplitude is shown in Table 1, which also shows the effects of various values of T_p. For a given value of T_p, each two-fold increase of A resulted in a corresponding two-fold increase of the local PSP peak value, as seen from the table.

Figure 3 shows the effects of changes in A or q upon somatic potential, with T_p fixed. Increases in A or q resulted in proportional increases in somatic potential. The curves in Figure 3 were computed for a synaptic location at a distance of $Z = 2$. The effects of different values of Z will be considered in a subsequent section.

An increase in T_p produced not only a delay in time-to-peak of the local dendritic PSP, but also resulted in a greater peak value, as seen in Figure 4. Note that there is not a linear relation between T_p and either the time-to-peak or the peak amplitude of the resulting PSP. This lack of linearity is made clearer by referring to Table 1. For example, an increase in T_p from 0.10 to 0.20 resulted in an increase from 0.2050 to 0.3900 in the time-to-peak, and an increase from 0.09677 to 0.1289 mV in the PSP amplitude for $A = 0.5$. Similar results were observed for the effects of T_p upon potential at the soma. However, a

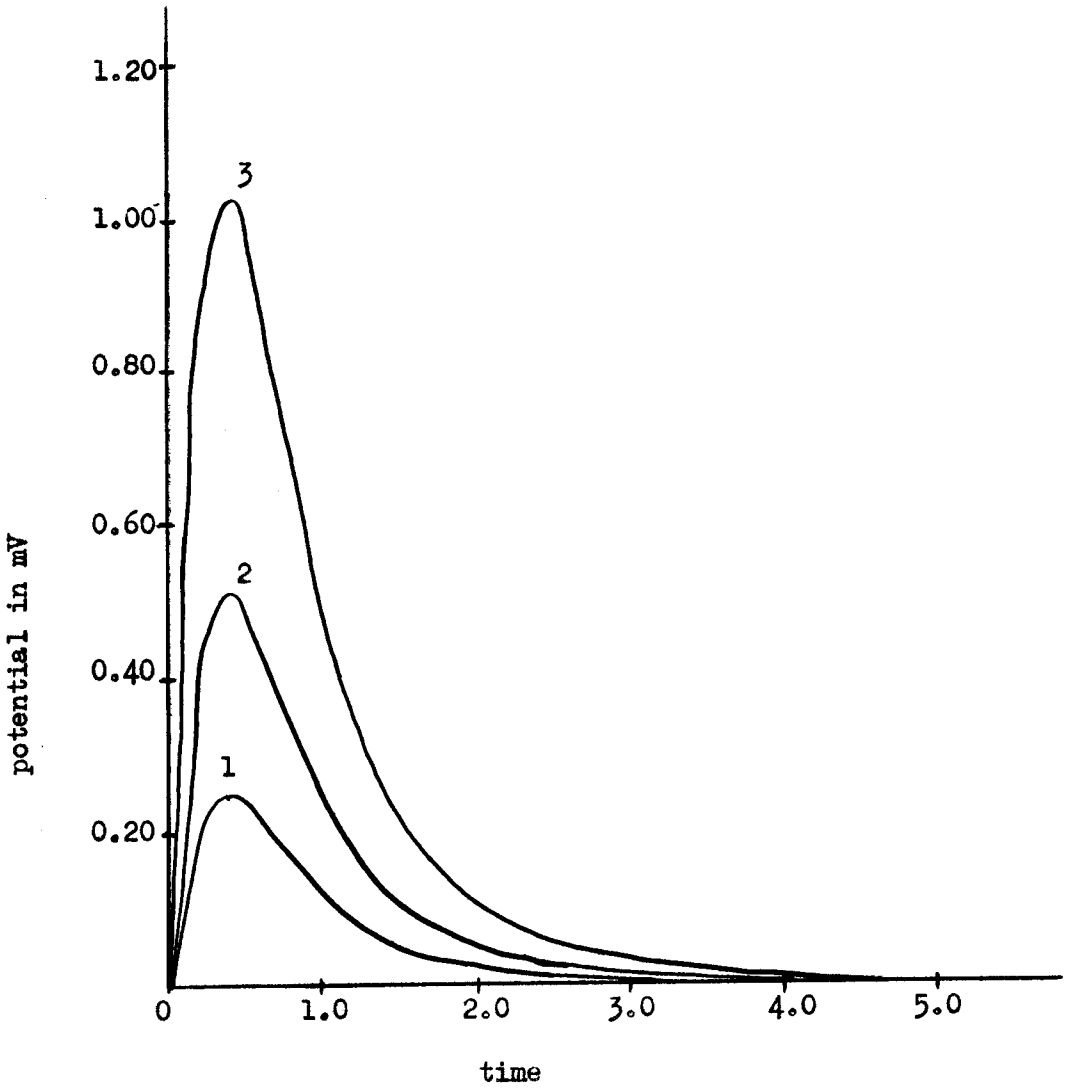

Figure 2. Local dendritic PSP as a function of A and q. For all curves, T_p=0.2, A=0.5. Curves 1, 2, and 3 correspond to respective q values of 2, 4, and 8.

Table 1. Local dendritic PSP parameters as a function of input potential transient parameters.

T_p[a]	Peak Time[b]	Peak[d]		
		A = 0.5[c]	A = 1.0	A = 2.0
0.05	0.1075	0.07073	0.1415	0.2829
0.10	0.2050	0.09677	0.1935	0.3871
0.15	0.3000	0.1149	0.2299	0.4597
0.20	0.3900	0.1289	0.2579	0.5158
0.25	0.4750	0.1403	0.2806	0.5613
0.30	0.5550	0.1498	0.2996	0.5993
0.35	0.6300	0.1579	0.3159	0.6317
0.40	0.7000	0.1650	0.3299	0.6598
0.45	0.7875	0.1711	0.3423	0.6846
0.50	0.8500	0.1766	0.3532	0.7064
0.55	0.9350	0.1815	0.3629	0.7259
0.60	0.9900	0.1859	0.3718	0.7435
0.65	1.073	0.1898	0.3796	0.7593
0.70	1.120	0.1934	0.3869	0.7737
0.75	1.200	0.1967	0.3934	0.7868
0.80	1.240	0.1997	0.3994	0.7988
0.85	1.318	0.2025	0.4050	0.8099
0.90	1.395	0.2050	0.4100	0.8200
0.95	1.425	0.2074	0.4147	0.8294
1.00	1.500	0.2096	0.4191	0.8382

[a]Time-to-peak of input potential transient, in normalized time units of T = t/5.

[b]Peak time of the resulting PSP, in normalized time units of T = t/5.

[c]A denotes amplitude of input potential transient.

[d]Peak values in mV.

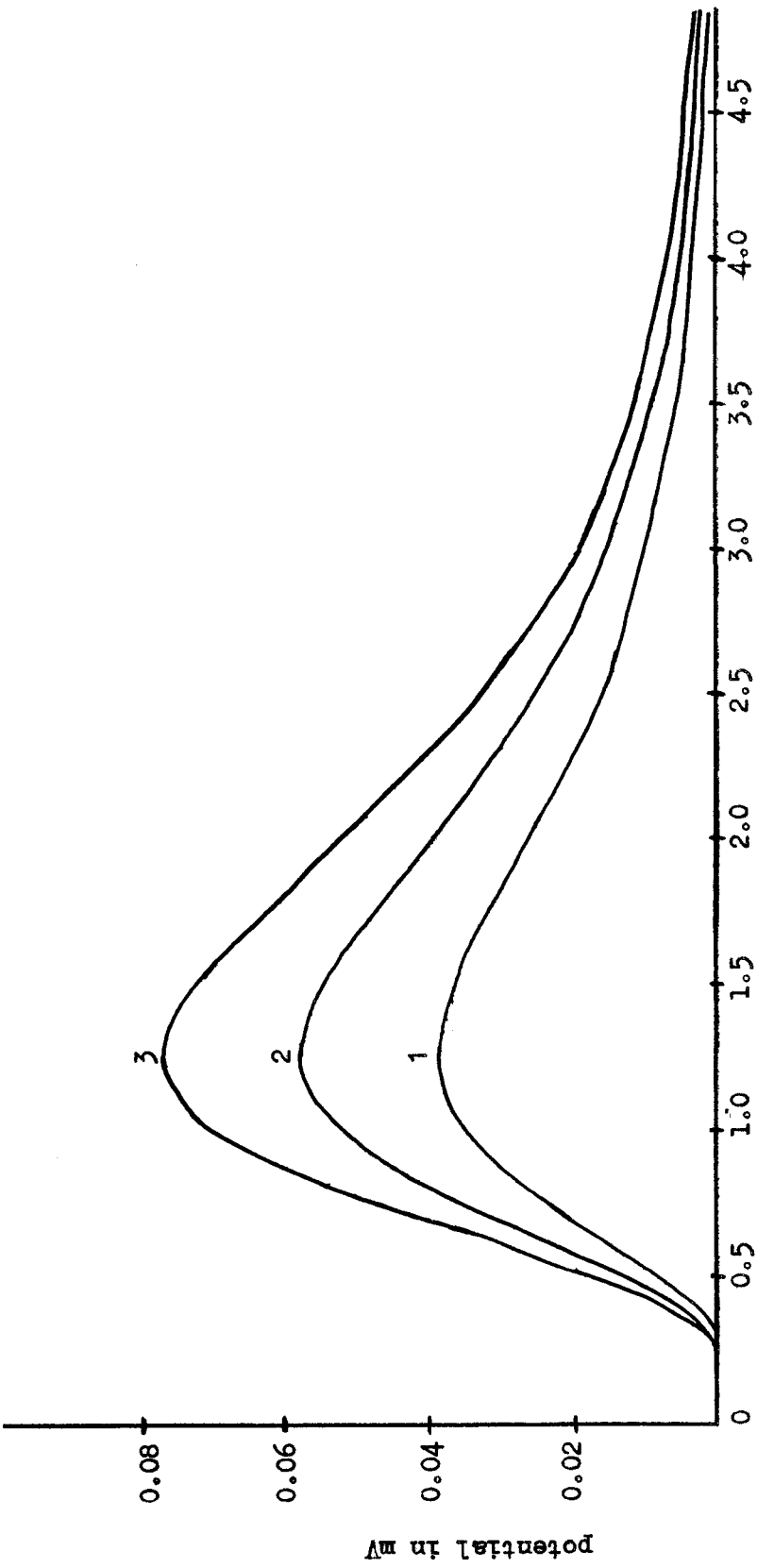

Figure 3. Somatic potential as a function of q. For all curves, z = 2, A = 0.5, T_p = 0.2. Curves 1, 2, and 3 correspond to q values of 4, 6, and 8, respectively.

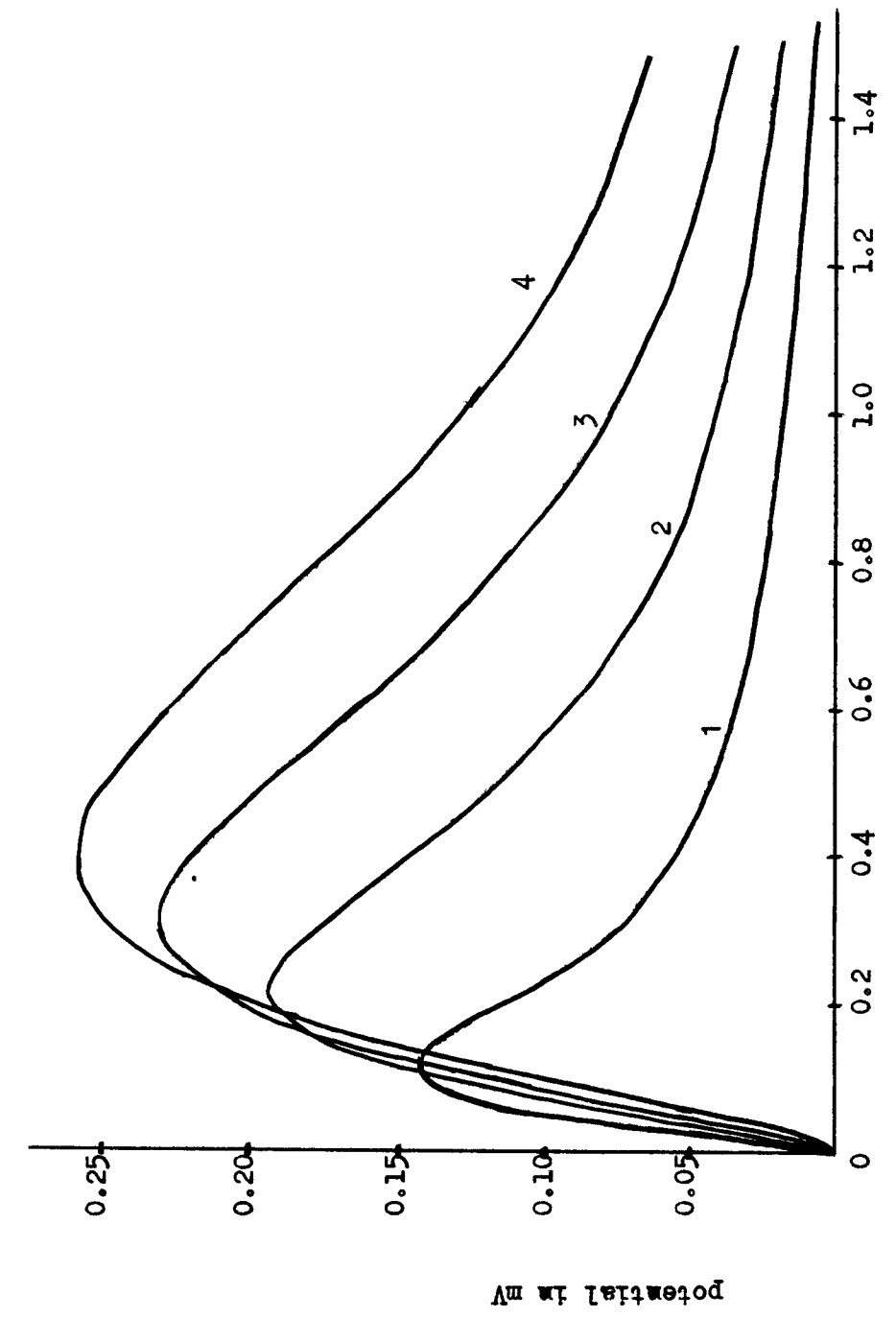

Figure 4. Shape of local dendritic PSP as a function of T_p. For all curves, q = 2, A = 0.5, z = 1. For curve 1, T_p = 0.05; for curve 2, T_p = 0.10; for curve 3, T_p = 0.15; for curve 4, T_p = 0.20.

given increment of T_p resulted in a proportionately larger increase in the peak potential at the soma than for the local PSP peak.

Figure 5 shows effects of T_p upon the somatic potential, and is drawn to the same scale as Figure 4, to facilitate comparison of the somatic potential curves with corresponding local PSPs in Figure 4. Each somatic PSP was shifted to the right for successive increases of T_p, as were the local PSPs. Of greater interest is the proportionately much greater increase in the peak value of the somatic PSP as opposed to the local PSP for a given increment of T_p. More detailed comparisons may be made with the aid of Table 2. For example, an increase of the corresponding peak values of local PSPs from 0.19353 to 0.25790 mV, while the somatic PSPs increased from 0.02169 to 0.06620 mV. The times-to-peak of successive somatic PSPs were also increased in greater proportion than those of the local PSPs for a given increment of T_p.

Effects of single activations at different locations

Comparisons of the effects of different locations with respect to attenuation of the PSP as it propagated to the soma are shown in Figure 6. The uppermost curve is the local dendritic potential, which was identical for all three locations. Although there are theoretical reasons for expecting changes in the peak amplitude of the local PSP as a function of distance from the soma, i.e., increased input resistance in smaller dendritic branches, the amplitude and time course of the unit input potential transient and the corresponding unit PSP were invariant with respect to location in the present study. The reason for keeping the form of the PSP identical for all locations is that it

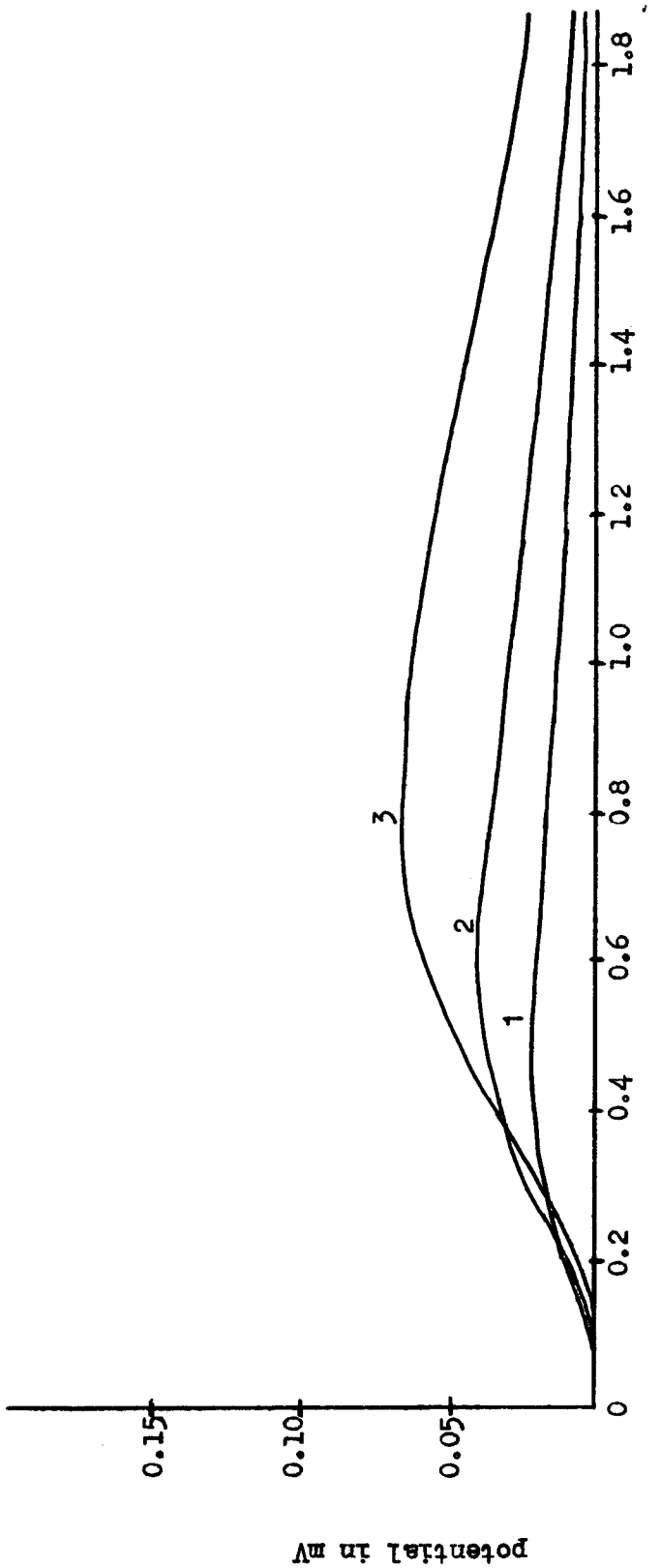

Figure 5. Somatic potential as a function of T_p. For all curves, A = 0.5, q = 2, z = 1. Curves 1, 2, and 3 correspond to T_p = 0.05, T_p = 0.10, and T_p = 0.20.

Table 2. Local and somatic potential peaks as a function of T_p and Z

T_p[a]	Z[b]	Local Dendritic Potential		Somatic Potential	
		peak time[a]	peak value[c]	peak time[a]	peak value[c]
.05	1	0.11	0.14143	0.44	0.02169
.05	2	0.11	0.14143	0.89	0.005469
.05	3	0.11	0.14143	1.36	0.001616
.10	1	0.21	0.19353	0.57	0.03966
.10	2	0.21	0.19353	1.01	0.01061
.10	3	0.21	0.19353	1.49	0.003181
.15	1	0.30	0.22987	0.70	0.05419
.15	2	0.30	0.22987	1.13	0.01521
.15	3	0.30	0.22987	1.61	0.004648
.20	1	0.39	0.25790	0.81	0.06620
.20	2	0.39	0.25790	1.25	0.01928
.20	3	0.39	0.25790	1.73	0.005996
.25	1	0.47	0.28063	0.91	0.07634
.25	2	0.47	0.28063	1.35	0.02287
.25	3	0.47	0.28063	1.84	0.007224

[a]Normalized time in units of $T = t/5$.

[b]Electrotonic distance from soma, in units of λ.

[c]Potentials in mV.

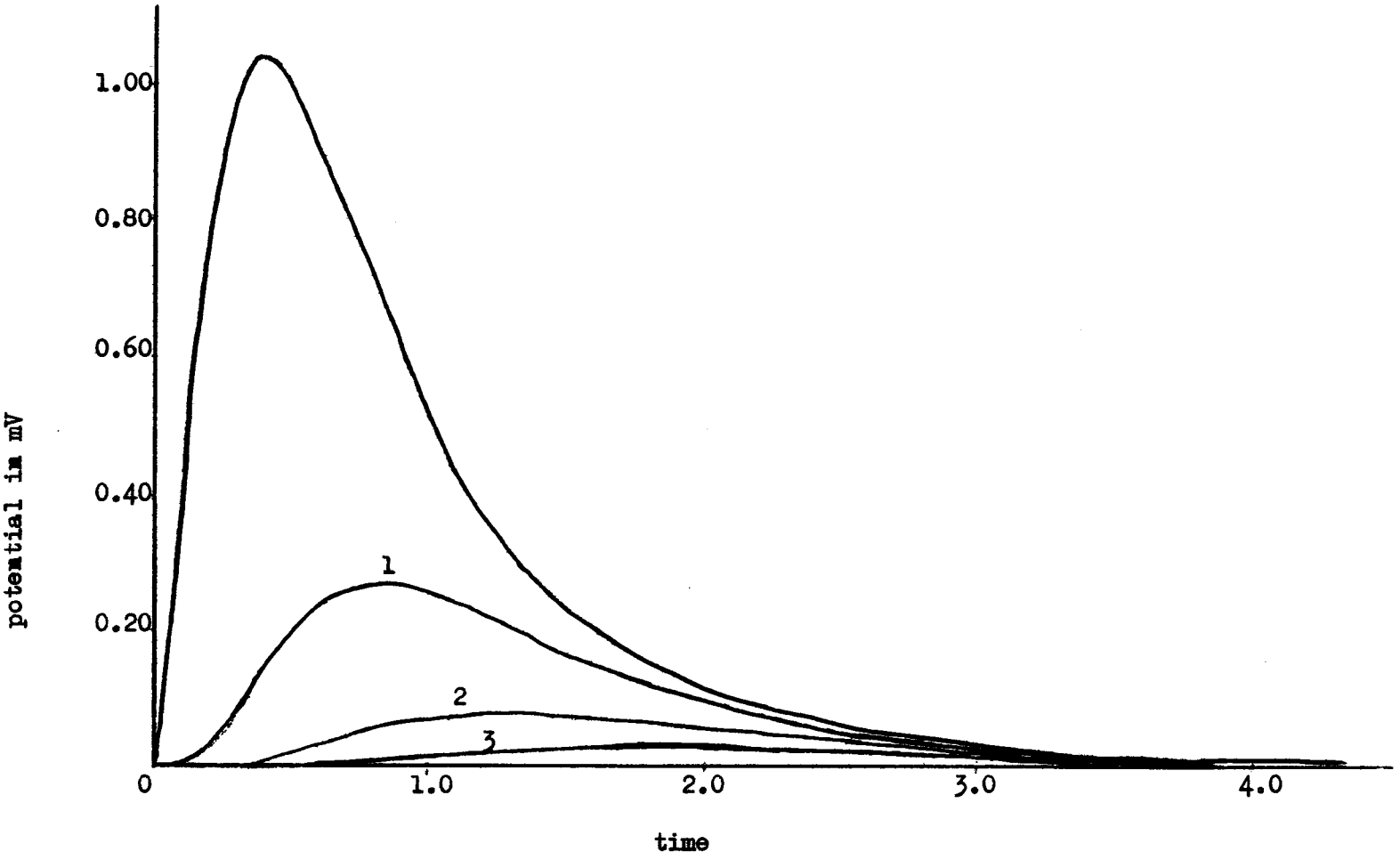

Figure 6. Attenuation of PSP as function of distance from soma. For all curves, T_p=0.2, A=0.5, q=8. Top curve is local dendritic PSP, which is identical for all 3 distances. Curves 1,2, and 3 correspond to respective distances Z=1,2, and 3.

is easier to compare the changes in somatic potential with reference to identically-shaped curves for PSPs located initially at different distances. Thus, the other three curves in Figure 6 show what happens to a PSP of the form shown by the top curve as it reaches the soma, whether it occurred at a distance of Z = 1, 2, or 3, corresponding to the numbered curves. It is evident that the greater the distance of a synaptic site from the soma, the greater the attenuation of an input at that site as it propagated to the soma. Note especially that a single PSP having a peak amplitude of about 1 mV occurring at Z = 3 decayed in propagation until the resulting somatic PSP had a peak amplutide of 0.0239 mV, so that such an isolated input produced a negligible effect upon somatic potential. Even a PSP of the same magnitude occurring at Z = 1 decayed to a somatic potential having a peak value of 0.2648 mV. It might seem that such small somatic peak values strengthen the idea mentioned previously that more remote dendritic inputs play in insignificant role in neuronal function. However, spatio-temporal summation of many such inputs can result in much larger changes in potential at the soma.

Before considering multiple activations, one further comparison will be made with reference to Figure 7. It is of interest to consider what quantal multiplier value would make a synapse at a more remote dendritic region approximately equivalent in efficacy to a more proximal synapse. For example, what quantal value would make a synapse at Z = 2 approximately as effective as a synapse at Z = 1, and having a quantal value of q = 2? Figure 7 shows that the somatic

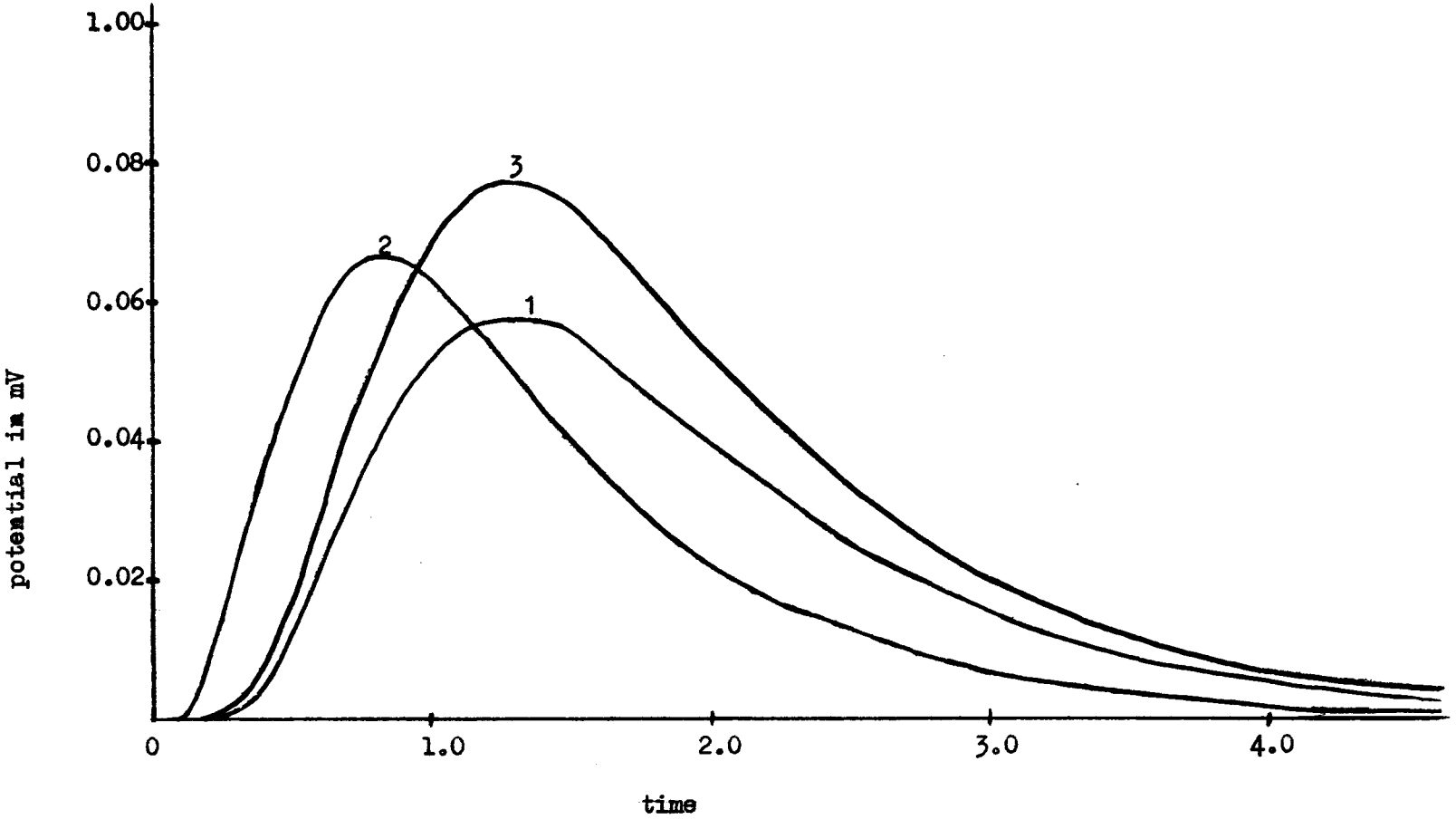

Figure 7. Comparisons of some combinations of z and q. For all curves, $T_p = 0.2$, A = 0.5. For curve 1, z = 2, q = 6. For curve 2, z = 1, q = 2. For curve 3, z = 2, q = 8.

potentials resulting from such single activations at Z = 2 having a quantal value of 6, produced a somatic PSP almost as large as the one produced by a single activation of a synapse at Z = 1 having a quantal value of 2. An activation at Z = 2 with q = 8 produced a peak larger than the one at Z = 1. An activation at Z = 2 with q = 7 would almost duplicate the somatic PSP for Z = 1, q = 2, except for its later peak time. At any rate, the model can show any number of such comparisons, and further mention will be made of these relations in the subsequent discussion of learning mechanisms.

Some simple temporal input patterns

Using his compartmental model, Rall (1964, 1965) showed that for single activations in compartments at different distances from the soma, the temporal ordering of the activations in the compartments had significant effects on the somatic potential. A temporal sequence of inputs in which synapses near the soma were activated first, followed by activations at successively more remote synapses, resulted in a computed somatic potential which showed a rapid rise and a very slow decline. A temporal sequence of inputs beginning at remote dendritic regions and progressing toward the soma resulted in a slower-rising curve with a much higher peak value. Simultaneous activations in all four regions resulted in a somatic potential curve having a rate of rise and a peak value intermediate to the cases above. The replication of the above simulation with the present model offers an interesting comparison between the two models. The present results go a step further and show that not only is there an optimum order of activations,

but that there is an optimum interval between the activations, with respect to producing the desired type of somatic potential change. Different sequences of inputs at three synapses, located at distances Z = 1, Z = 2, and Z = 3, were studied. In all cases considered, the values q = 5, A = 0.5, and T_p = 0.2 were used. Curve 1 of Figure 8 shows the theoretical somatic potential resulting from one simultaneous activation at all three synapses. Curve 2 shows the somatic potential resulting from an activation at Z = 1, followed by an activation at Z = 2, followed by an activation at Z = 3, with an interval of 0.5 between the activations. Curve 3 shows the same order of activations, but with an interval of 1.5 between the activations. All three peaks due to the individual activations can be detected in curve 3, due to the longer interval between activations, while they are not observed in the other two curves. Both of the curves computed for the activation order 1-2-3 have peaks lower than the curve computed for simultaneous activations. Both of these curves also have peaks occurring slightly before the peak of curve 1. The tail of curve 3 remains above the tails of curves 1 and 2. Further details are given in Table 3. These results, while not an exact duplication, are in good agreement with those obtained by Rall, whose theoretical calculations are being experimentally corroborated. Figure 9 shows further agreement, with respect to the opposite order of activation.

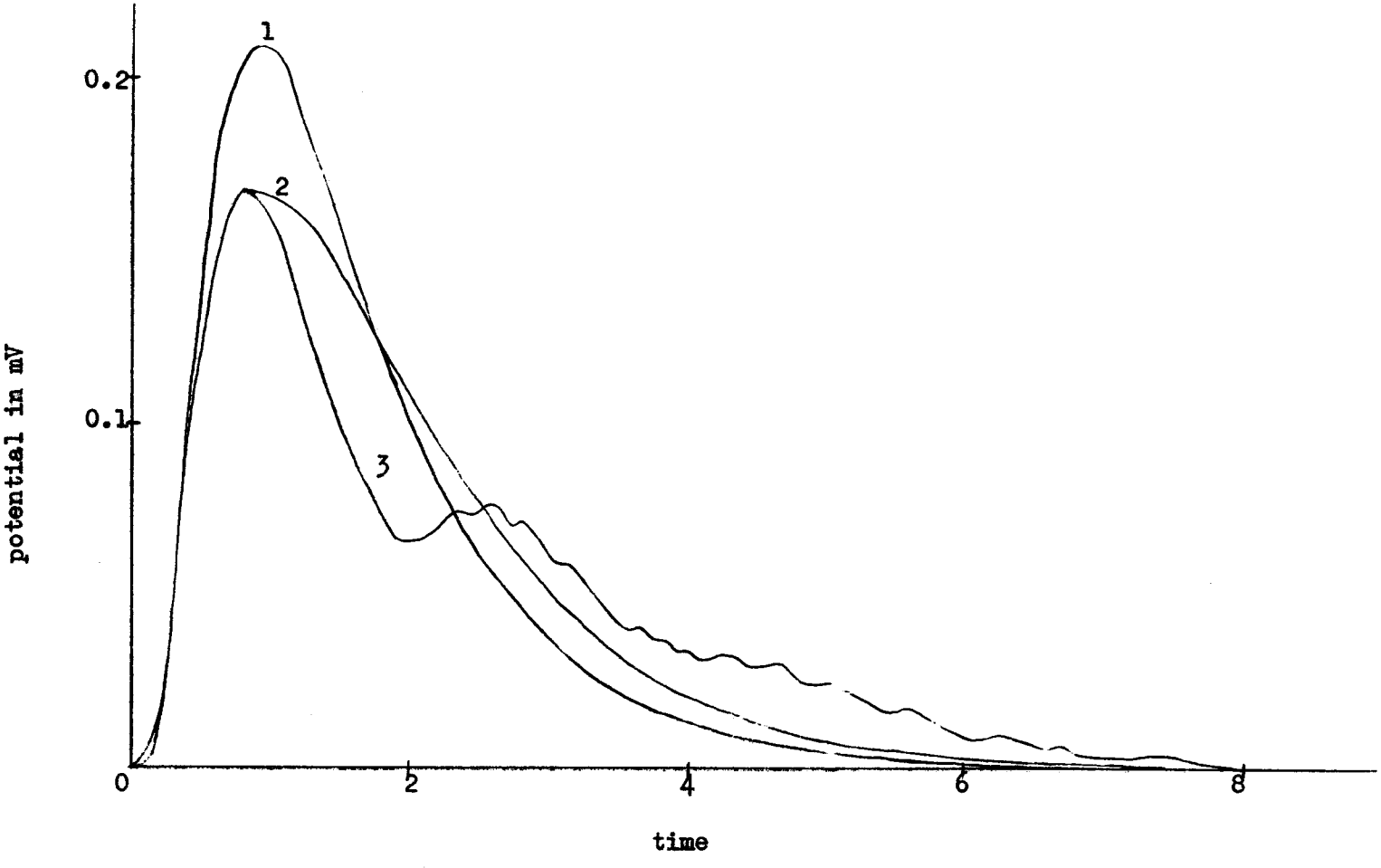

Figure 8. Effect of activation sequence and interactivation interval upon somatic potential. For all curves, q=5, T_p=0.2, A=0.5, synapse 1 at Z=1, synapse 2 at Z=2, synapse 3 at Z=3. Curve 1: simultaneous activation at all 3 synapses. Curves 2 and 3: activation sequence 1-2-3 for the respective interactivation intervals 0.5 and 1.5.

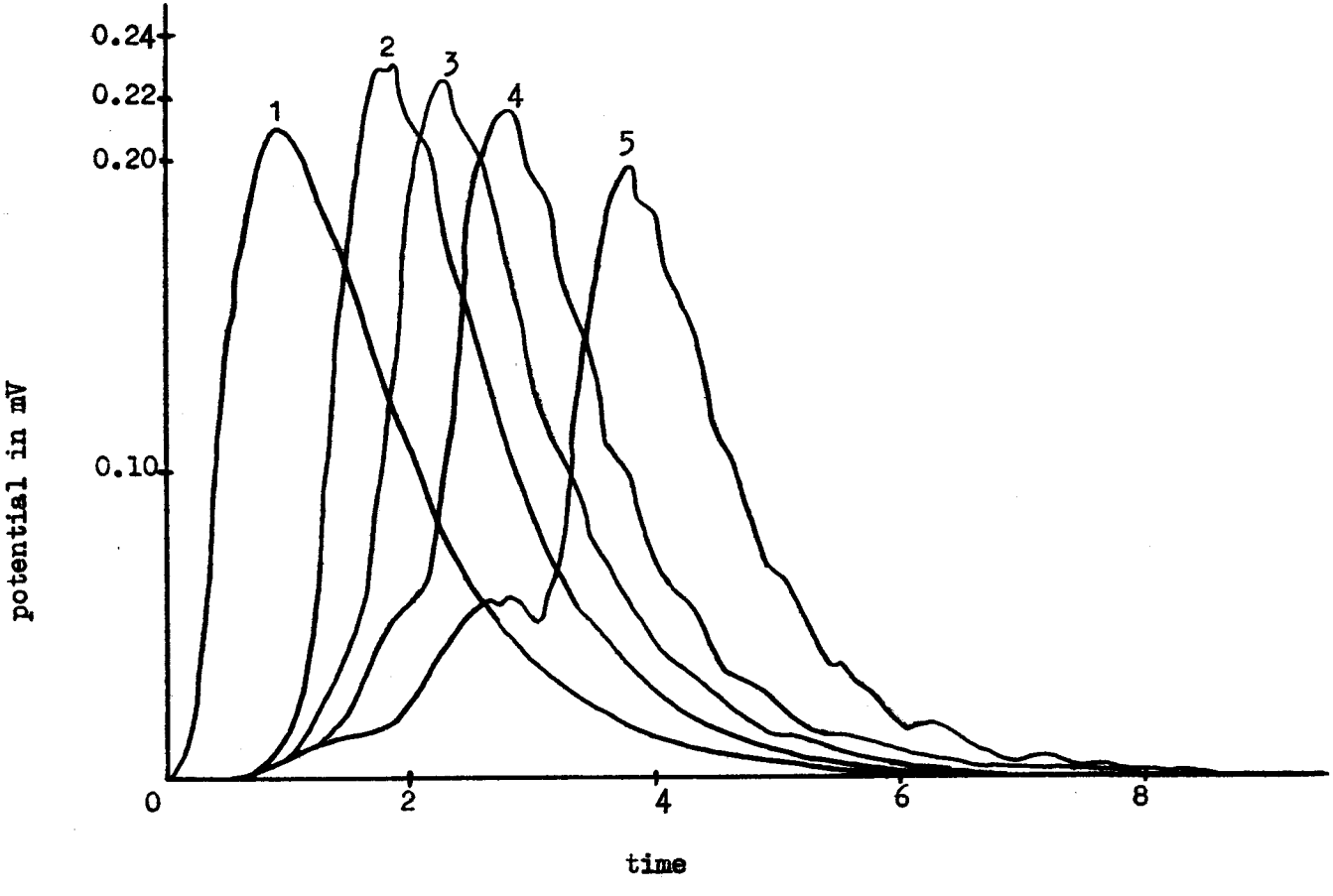

Figure 9. Effect of reversed activation sequence and interactivation interval upon somatic potential. For all curves, q=5, T_p=0.2, A=0.5, synapse 1 at Z=1, synapse 2 at Z=2, synapse 3 at Z=3. Curve 1 shows effect of simultaneous activation at all 3 synapses. Curves 2, 3, 4 and 5 show activation sequence 3-2-1 for the respective interactivation intervals 0.5, 0.75, 1.00 and 1.5.

Table 3. Comparison of effect of activation sequence and interactivation intervals for single activations at three synapses located at Z = 1, Z = 2, Z = 3

Case[a]	Interactivation Interval[b]	Somatic Potential	
		Time to peak[b]	Peak value[c]
A	0	0.9	0.2077
B	0.25	1.0	0.1855
B	0.5	0.9	0.1673
B	1.5	0.8	0.1655
C	0.25	0.14	0.2243
C	0.5	0.19	0.2268
C	0.75	0.23	0.2250
C	1.00	0.28	0.2137
C	1.5	0.38	0.1970

[a]In all cases, $T_p = 0.2$, A = 0.5, and q = 5. Case A denotes simultaneous activation at all 3 synapses, case B denotes activation in the order 1-2-3, and case C denotes activation sequence 3-2-1.

[b]Normalized time units of T = t/5.

[c]Potential in mV.

Curve 1 of Figure 9 is the same as curve 1 of Figure 8, i.e., the result for three simultaneous activations, and is reproduced in Figure 9 to facilitate comparisons. Curves 2, 3, 4, and 5 were computed for an activation at Z = 3, followed by an activation at Z = 2, followed by an activation at Z = 1. Curves 2, 3, and 4 all have peaks which occur later, are sharper, and are higher than that of curve 1. Curve 5 has a lower peak, which is due to the long interval between activations. The best interactivation interval of the values tested was 0.5, which corresponds to curve 2. This optimum interactivation interval depends upon the propagation velocity of the PSP. It can be seen intuitively that this optimum situation occurs when each successive peak arrives so that a new activation is added to the peak of the preceding PSP instead of to a lower point on the tail, thus giving maximal temporal summation. Curve 2 of Figure 9 comes very close to attaining the maximum possible amount of temporal summation under the conditions studied. The peak amplitudes of somatic potentials resulting from single activations at only a single synapse located at Z = 1, Z = 2, or Z = 3 (computed in a separate simulation) were 0.1655, 0.0480, and 0.0150 mV. The sum of these values is 0.2285 mV, which differs negligibly from the peak value of 0.2268 mV for curve 2. In the same previous simulation, the times-to-peak of the somatic potentials for the single activations at a single synapse were 0.8 for Z = 1, 1.2 for Z = 2, and 1.7 for Z = 3. These delays in the time-to-peak correspond to the optimum interval of 0.5 in curve 2. Thus, both the order of activations and the interval between activations have significant effects upon the somatic potential.

Repeated activations at a single synaptic site

Each of the variables investigated above for single activations at a synapse was also investigated for repeated activations at a synapse. The effects of quantal values upon somatic potential are illustrated in Figure 10. Each curve is the calculated somatic potential for five activations at intervals of 1.0, for a synaptic site at Z = 1, with T_p = 0.2, A = 0.5. Each curve is twice the height of the one below it, showing that the linear relation between q and somatic potential still holds for these multiple activations, which is to be expected since q multiplies the whole input potential transient function. However, some interesting effects were observed when the other parameters were studied for cases of repeated activations.

Figures 11, 12, 13, and 14 show comparisons of effects of interactivation interval and distance from soma upon somatic potential. Figure 11 shows calculated somatic potentials for five activations occurring at Z = 1, Z = 2, or Z = 3, at intervals of 3.0. For all curves, T_p = 0.2, q = 8, and A = 0.5. Due to the long interval between activations, the degree of temporal summation was slight in all three cases. An interesting effect observed in these curves was the appearance of extra small peaks, in addition to the five large peaks corresponding to the five activations. Discussion of these extra peaks will be deferred to a subsequent section.

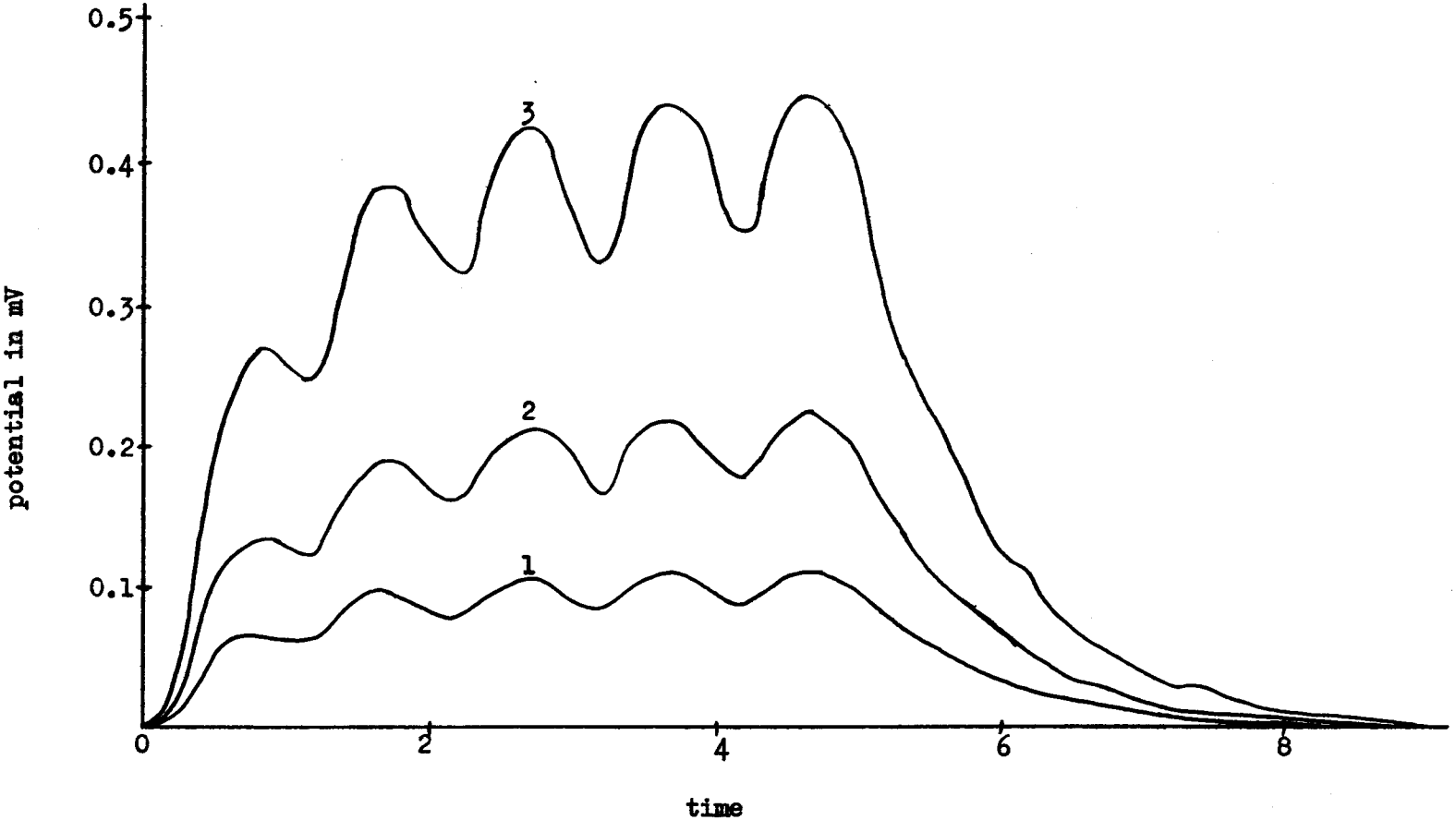

Figure 10. Somatic potential as a function of q for multiple activations. For all curves, A=0.5, T_p=0.2. For curve 1, Z=2, q=2. For curve 2, Z=1, q=2. For curve 3, z=1, q=4.

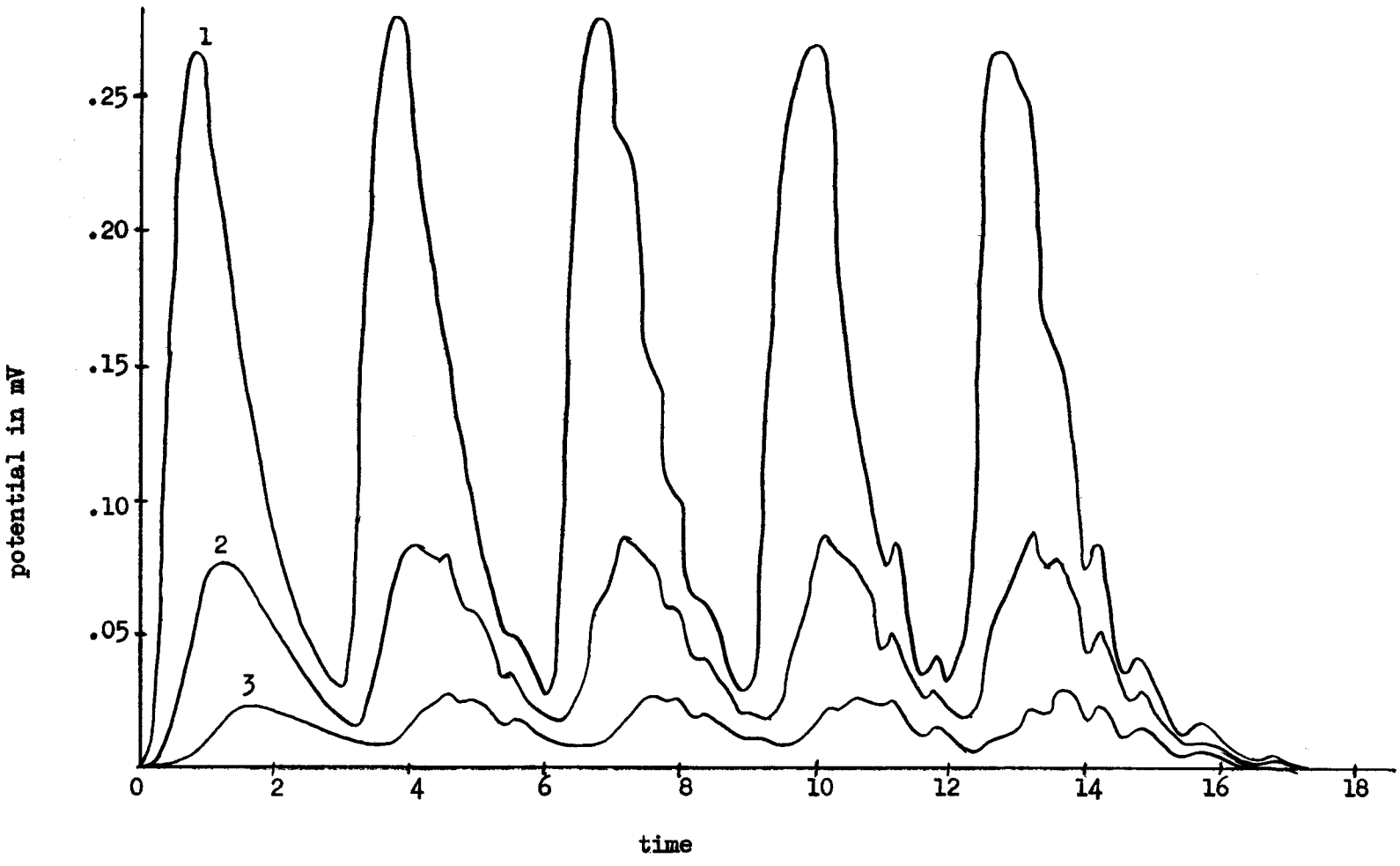

Figure 11. Somatic potential as a function of Z, for interactivation interval of 3.0. For all curves, q=8, T_p=0.2, A=0.5. Five activations for each curve. Distances from soma are Z=1, 2, 3 corresponding to numbers on the curves.

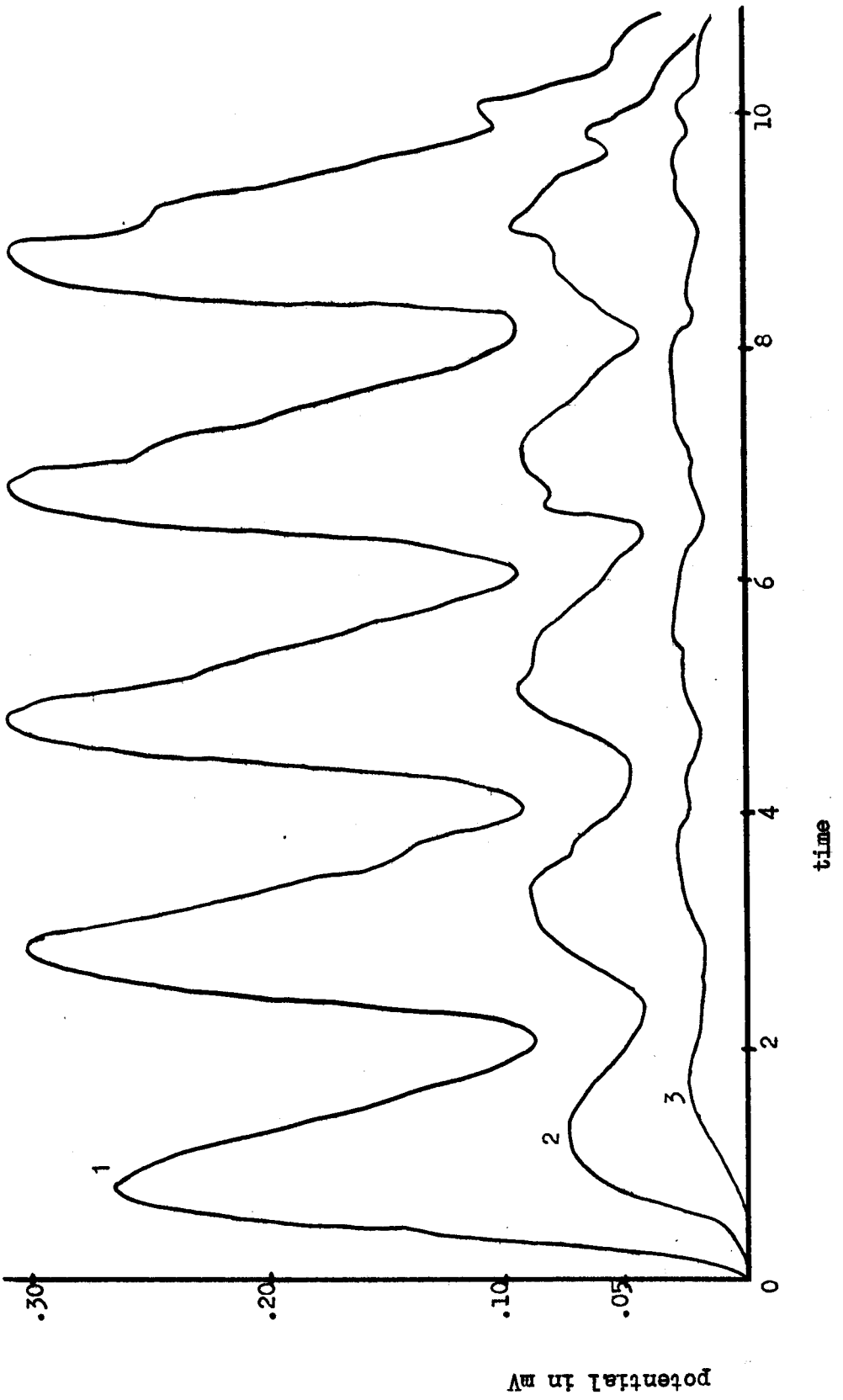

Figure 12. Somatic potential as a function of Z, for interactivation interval of 2.0. For all curves, q=8, T_p=0.2, A=0.5. Five activations for each curve. Distances from soma are Z=1, 2, 3, corresponding to numbers of the curves.

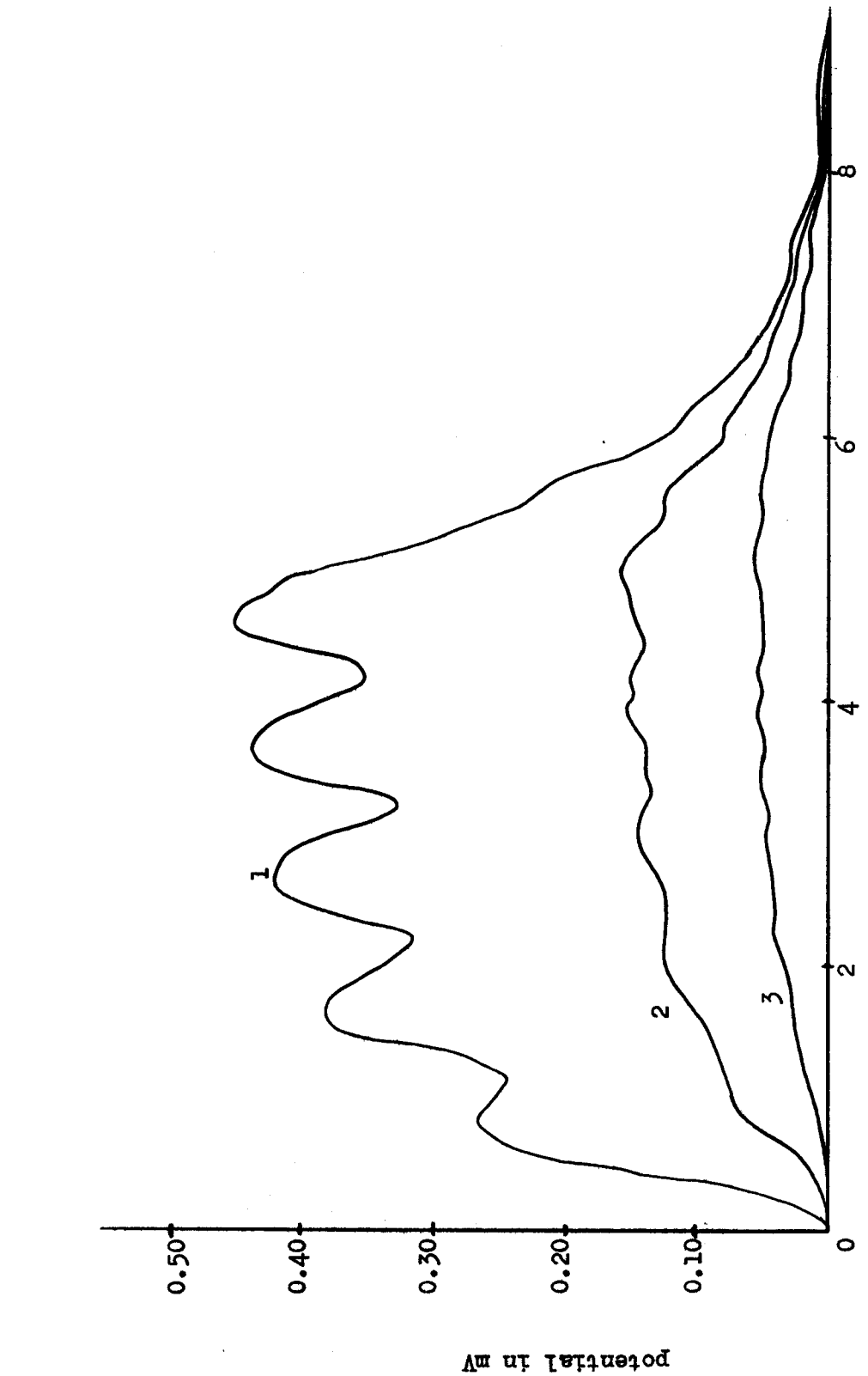

Figure 13. Somatic potential as a function of Z, for interactivation interval of 1.0. For all curves, q=8, T_p=0.2, A=0.5. Five activations for each curve. Distances from soma are Z=1, 2, 3, corresponding to numbers on the curves.

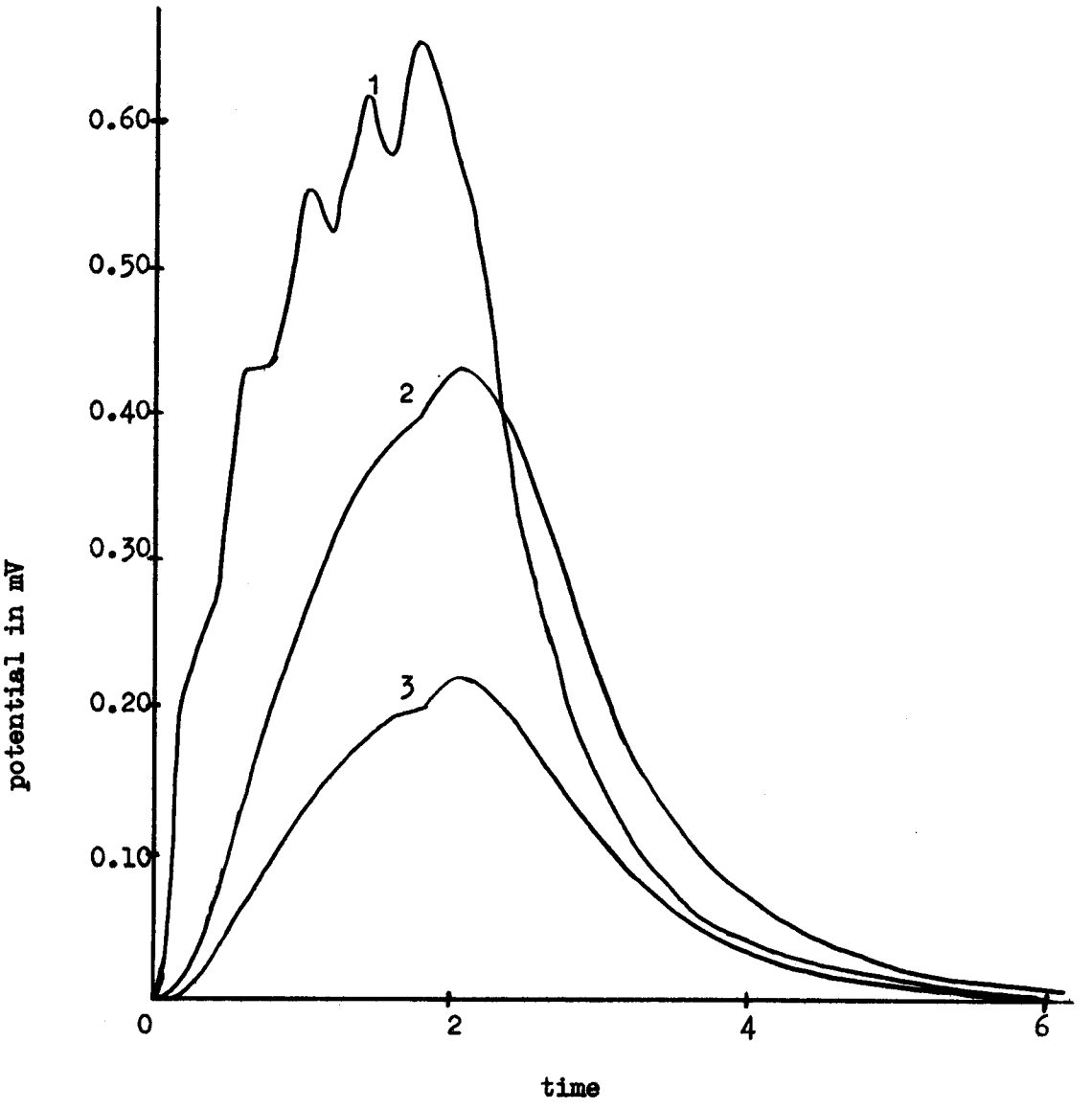

Figure 14. Effects of short interactivation interval upon temporal summation. For all curves, T_p=0.2, A=0.5. Curve 1 shows local PSP for Z=1, q=2. Curve 2 shows somatic potential for Z=1, q=4. Curve 3 shows somatic potential for Z=1, q=2.

Figure 12 shows calculated somatic potentials for five activations at Z = 1, Z = 2, Z = 3, at intervals of 2.0. All other parameters are the same as for Figure 13. The smaller interactivation intervals resulted in a greater amount of temporal summation for each curve, as evidenced by the progressive increases in amplitude of the peaks. Extra small peaks may be seen again in these curves, but are not as pronounced as in the corresponding curves of Figure 11. Note the small but almost constant level of potential resulting from activations at Z = 3.

Figure 13 shows the results of the same calculations as for Figures 11 and 12, with the only difference being an interactivation interval of 1.0 in this case. The shorter interval resulted in a much greater degree of temporal summation. For example, the highest peak value for curve 1 of Figure 12 was 0.3099 mV, while a value of 0.4487 mV was calculated for the corresponding curve 1 of Figure 13.

In Figure 14, two calculated somatic potentials for an interactivation interval of 0.4 are shown, with all other parameters being identical to those used in calculations for the related figures. The two somatic potential curves shown correspond to values of q = 2 and q = 4, both at distance Z = 1. In addition, the local dendritic PSP curve for Z = 1 and q = 2 is shown. The temporal summation of local PSPs is very great in comparison to the other curves. Note that the curve for q = 4 in Figure 14 rises to a peak which is almost as high as that for q = 8 in Figure 13. Also, except for a slight hump to the left of the peak, both curves 2 and 3 in Figure 14 are smooth, with no

evidence of the five separate peaks due to the five activations. In all computations related to Figure 11, 12, 13, and 14, temporal summation of local PSPs occurred to some degree, but to a far greater degree for the cases where an interactivation interval of 0.4 was used. Thus a maximal peak value of somatic potential may be obtained for inputs at a single synapse by finding an optimum interval between activations. The results show that as the interval between activations decreased, the peak value of somatic potential increased. This interval cannot generally be less than about 1 msec (corresponding to an interactivation interval of 0.2 in the present model) since the absolute refractory period of a neuron is around 1 msec, which sets a limit on the interval between arriving impulses at a single synaptic site (Stevens, 1966). In the present model, the interactivation interval of 0.4 corresponds to a 2 msec interval, or to an input frequency of 500 impulses per second.

Figure 15 shows somatic potentials computed for five activations at $Z = 0.25$ and $Z = 0.5$, with $q = 4$ and $q = 8$. The interactivation interval used was 1.0, the same as in Figure 13; the values of T_p and A were also the same. The resulting somatic potential was much larger than that for activations at greater distances from the soma. A value of $Z = 0.25$ may be considered to be a somatic region, in terms of the present model.

Changing the value of T_p produced marked effects of the somatic potentials calculated for five activations at a single synaptic site. Figure 16 shows two curves resulting from such calculations, with $T_p = 0.1$, and all other parameters identical to those of Figure 13.

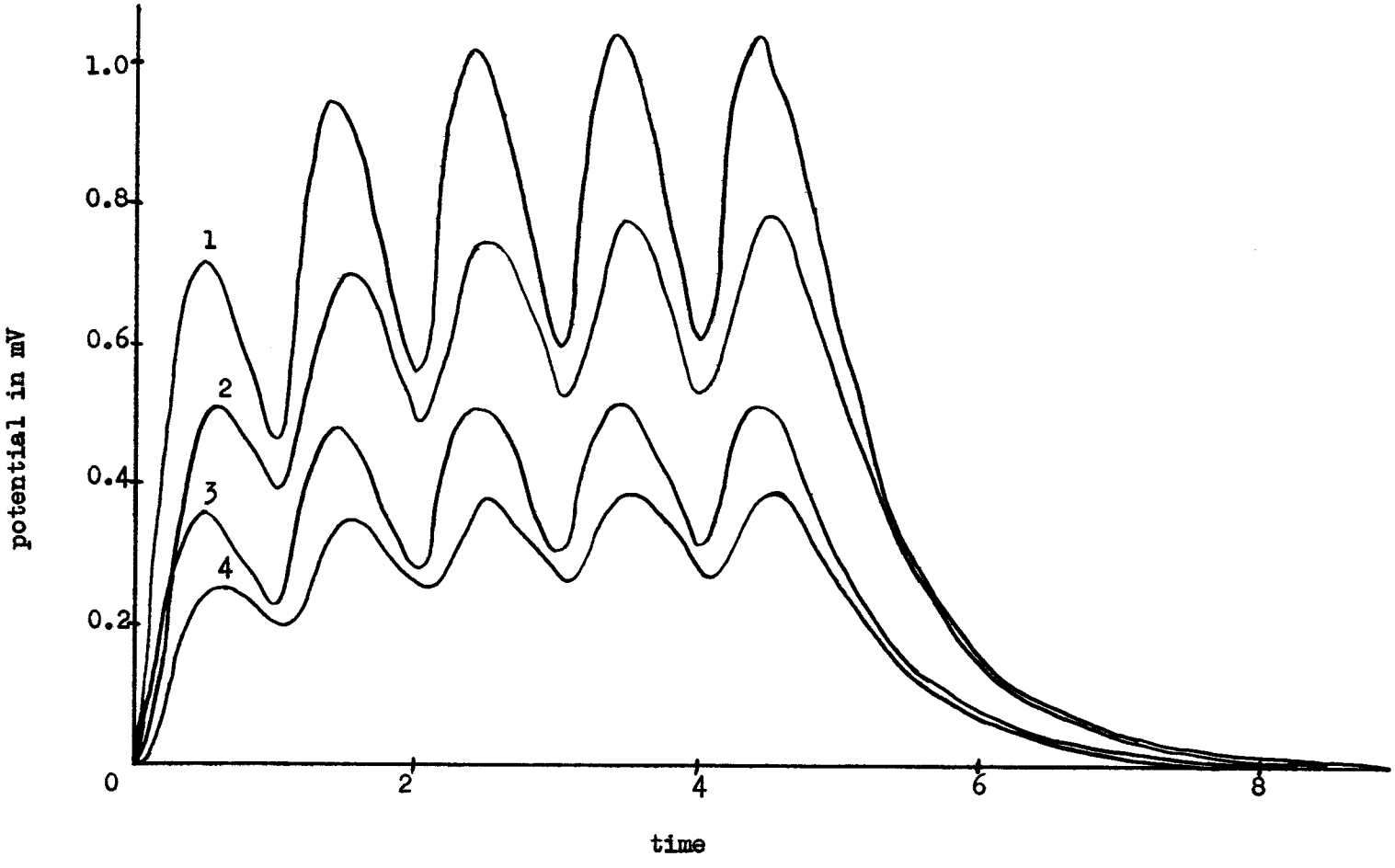

Figure 15. Somatic potential for activations near soma. Five activations at intervals of 1.0. For all curves, T_D=0.2, A=0.5. For curve 1, Z=0.25, q=8. For curve 2, Z=0.5, q=8. For curve 3, Z=0.25, q=4. For curve 4, Z=0.5, q=4.

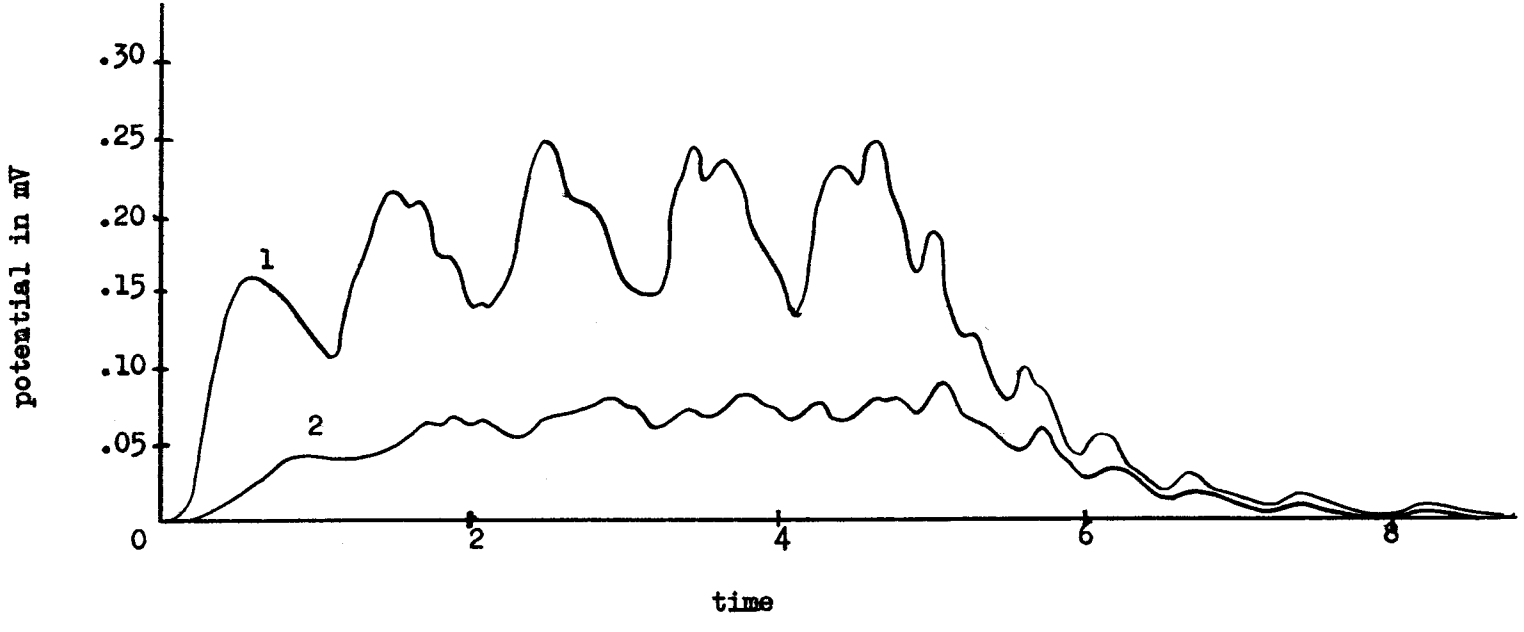

Figure 16. Somatic potential as a function of T_p and Z. For both curves, T_p=0.1, A=0.5. For curve 1, Z=1, q=8. For curve 2, Z=2, q=8. Five activations at intervals of 1.0 for each curve.

Several extra peaks are seen in curve 1 of Figure 16, while none are present in curve 1 of Figure 13. In curve 2 of Figure 16, the five primary peaks are almost obscured by the extra peaks. To facilitate comparison, curves 1 from both Figures 13 and 16 are reproduced in Figure 17. Not only are the extra peaks conspicuous, but decreasing T_p reduced the amplitude of the somatic potential by a significant amount. The reduction in peak amplitude for five activations was proportionately greater than for a single activation, as seen by comparison of the curves for $T_p = 0.1$ and 0.2 in Figures 17 and 4. In Figure 4, the curve for $T_p = 0.1$ had a peak value of about 0.194 mV, while the peak for $T_p = 0.2$ was about 0.257 mV. The largest peak for the curve corresponding to $T_p = 0.1$ in Figure 17 was around 0.125 mV, while the largest peak for $T_p = 0.2$ was around 0.225 mV.

Figure 18 shows computed somatic potentials for 20 activations at intervals of 1.0 for Z = 1 and Z = 2. In both cases, q = 10, A = 0.5, and $T_p = 0.2$. Extra peaks are numerous and of appreciable magnitude in both curves. In the curve for Z = 1, some extra peaks are almost as large as 0.1 mV, which definitely is of significance in experimentally recorded PSP profiles. Note that the latter parts of both curves look almost as if they were produced by random patterns, yet they were generated by a deterministic model. The twenty peaks corresponding to the separate activations can still be identified and counted in the top curve, but cannot be in the bottom curve. At this point, it can be stated that the appearance of extra peaks depends upon the shapes of the individual PSPs and upon the interactivation interval. Further discussion will show how these variables produce the extra peaks.

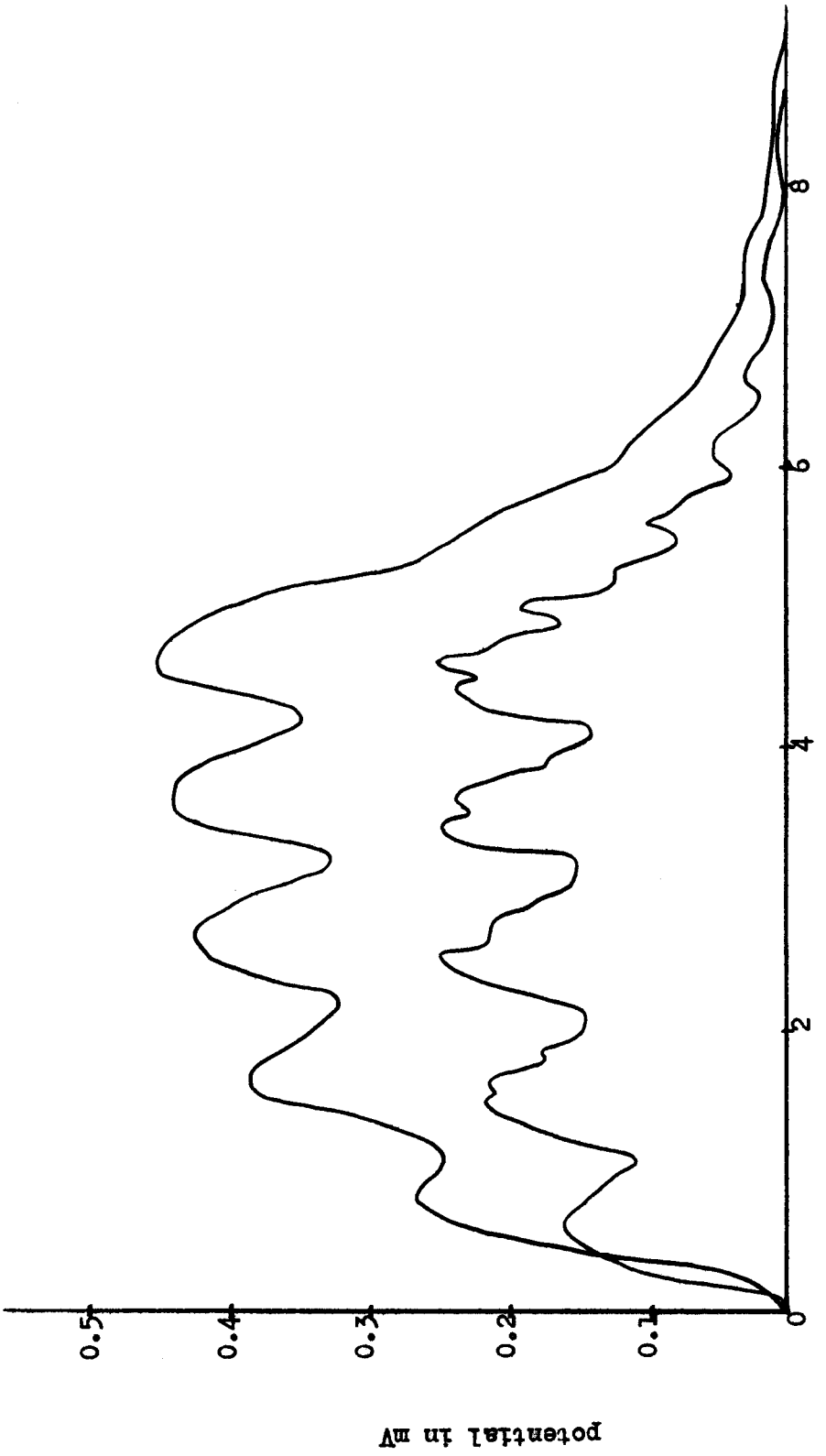

Figure 17. Somatic potential as a function of T_p for five activations. For both curves, A=0.5, Z=1, q=8. For the upper curve, T_p=0.2. For the lower curve, T_p=0.1.

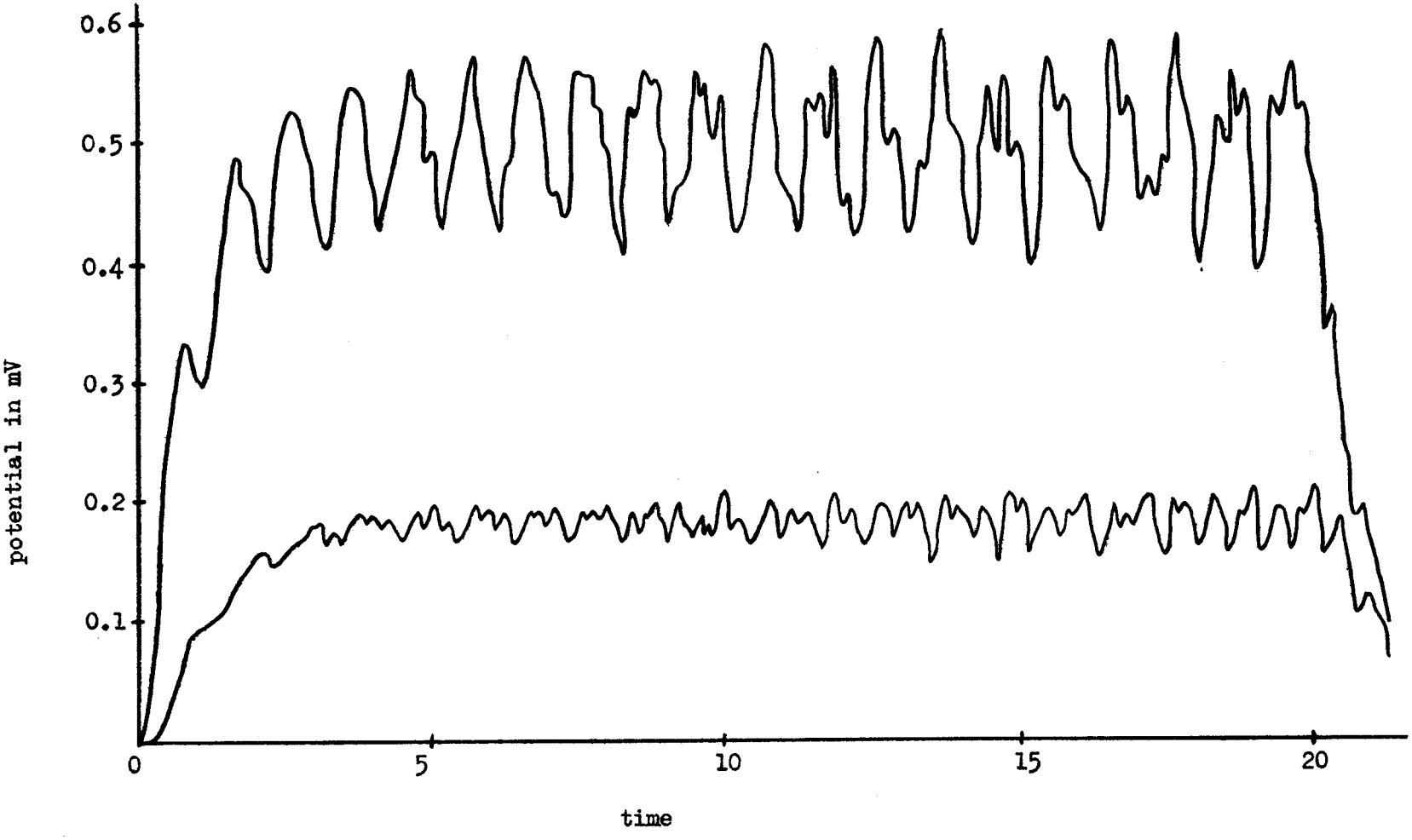

Figure 18. Twenty activations at two different distances from the soma. For both curves, T_p=0.2 A=0.5, q=10, with interactivation interval of 1.0. For upper curve, Z=1. For lower curve, Z=2.

Some complex activation patterns

Activation patterns involving repeated activations at multiple synaptic sites will be termed complex activation patterns, to distinguish them from the simpler situations considered above. A few examples of complex activation patterns will be presented to show that the basic relations among the various parameters apply equally well to complex activation patterns.

Figure 19 shows calculated somatic potentials for 10 activations at Z = 2 at intervals of 2.0, beginning at T = 0, and 5 activations at Z = 1, at intervals of 1.0, beginning at T = 2. Both synapses were on the same dendritic cylinder. The synapse at Z = 2 had a fixed value of q = 5 for both curves. For the top curve, the synapse at Z = 1 had q = 6, while for the lower curve, the same synapse had q = 4. For both curves, T_p = 0.2 and A = 0.5. The effects of increasing the quantal number at one synapse are clearly illustrated by the figure. Both curves are indistinguishable up to the point of divergence, corresponding to the beginning of activations at Z = 1, and after the point of convergence. Numerical differences between the curves for the latter region were too small to illustrate in the figure; there were no numerical differences between the curves for the initial portion, until activations began at Z = 1.

A second example of the effect of increasing the quantal number at a single synaptic site is shown in Figure 20, which shows somatic potentials for 10 activations at Z = 3 on one dendritic cylinder at intervals of 0.6 starting at T = 0, 5 activations at Z = 1 on a

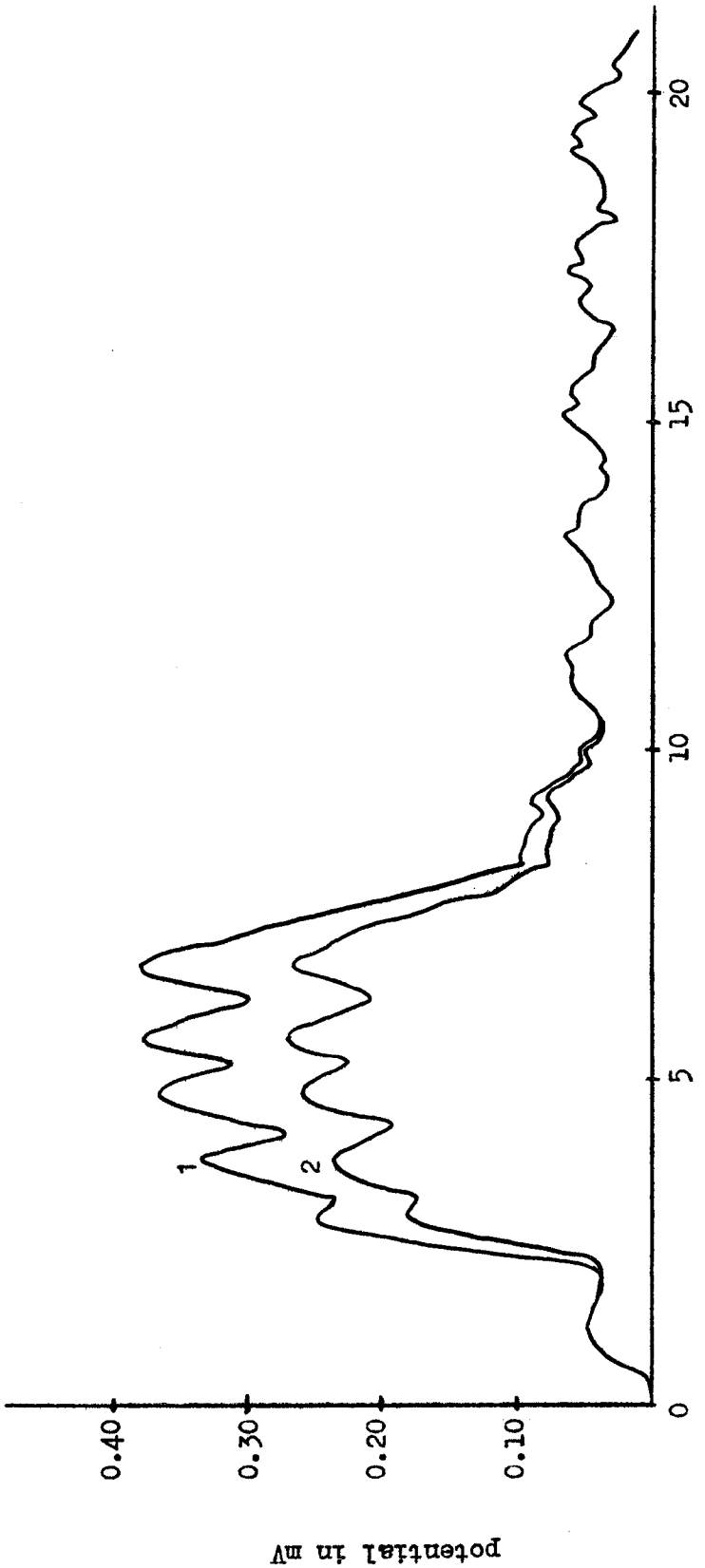

Figure 19. Repeated activations at two synapses on one dendritic cylinder. Somatic potentials for 10 activations at Z-2, at intervals of 2.0, beginning at T=0, and 5 activations at Z=1, at intervals of 1.0, beginning at T=2. For both curves, q=5 for synapse at Z=2. For curve 1, q=6 for synapse at Z=1; for curve 2, q=4 for the same synapse. For both curves T_p=0.2, A=0.5.

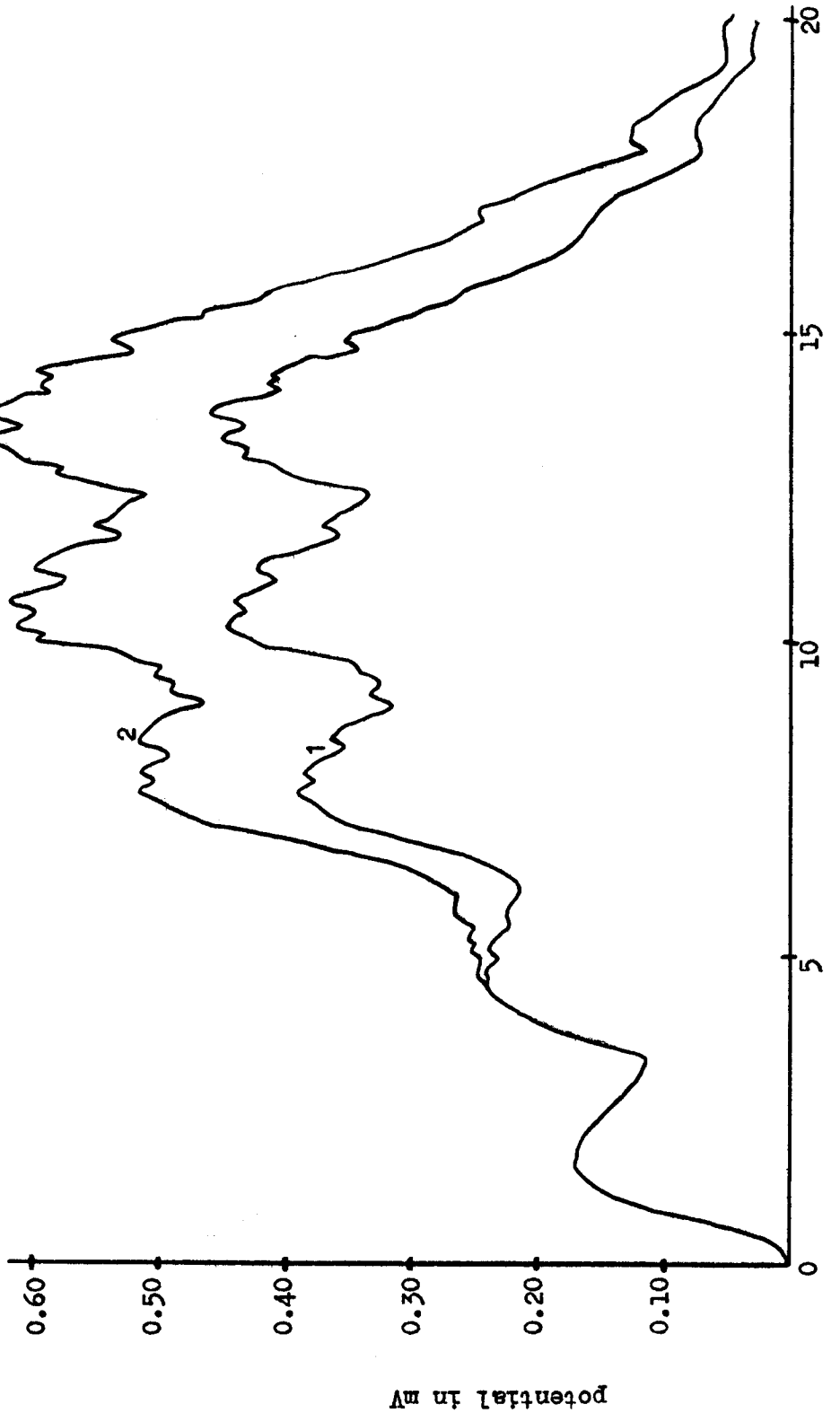

Figure 20. Effects of increased quantal amount of transmitter upon PSP. For curve 1, q=5 for all synapses. For curve 2, q was changed to 10 for synapse on 2nd branch. Other parameters identical for both curves.

second dendritic cylinder at intervals of 0.5 starting at T = 2.0. For both curves, T_p = 0.2, A = 0.5. For curve 1, q = 5 for all synapses. Changing q to 10 for the synapse at Z = 2 on the second cylinder produced curve 2. Changing the value of q at one synapse by 5 thus changed the peak somatic potential from around 0.45 to 0.65 mV.

Figure 21 shows the most complex patterns considered in the study. The results of these two complex activations were in agreement with previously calculated effects of simpler patterns. Each curve results from 10 activations at 5 synaptic sites on a total of 3 dendritic cylinders. In both cases, T_p = 0.2, A = 0.5, and q = 5 for all synapses. For curve 1, the following inputs were used: 10 activations at intervals of 0.6, beginning at T = 5.0 for Z = 0.5 on the first cylinder; 10 activations at intervals of 1.5, beginning at T = 0 for Z = 3.0 on the same cylinder; 10 activations at intervals of 0.8 beginning at T = 5.0 for Z = 1.0 on a second cylinder; 10 activations at intervals of 1.0 beginning at T = 1.0 for Z = 2.0 on a third cylinder. The net effect of this pattern was simply to provide initial activations at more remote dendritic regions, followed by bursts of activations nearer the soma. For curve 2, the activation patterns for the synapses on the first two cylinders were reversed. The synapse at Z = 0.5 on the first cylinder had 10 activations at intervals of 1.5, beginning at T = 0; the synapse at Z = 3.0 on the same cylinder had 10 activations at intervals of 0.6, beginning at T = 5; the synapse at Z = 1.0 on the second cylinder had 10 activations at intervals of 1.0, beginning at T = 0; the synapse at Z = 3.0 on the same cylinder had 10 activations

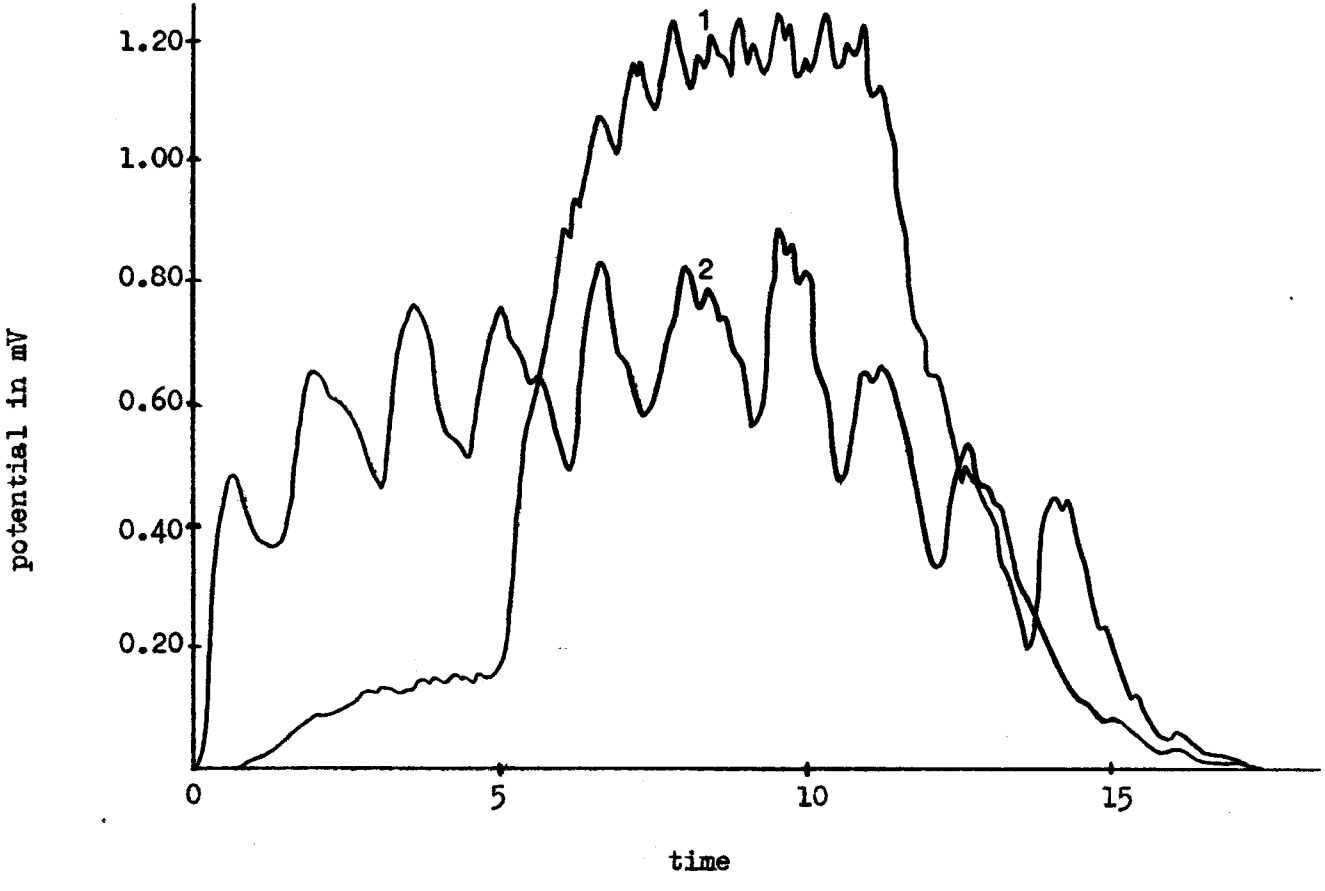

Figure 21. Order effects for bursts of activations. Curve 1 represents activations at remote regions, followed by bursts nearer soma. Curve 2 represents initial bursts near soma, followed by activations at remote regions.

at intervals of 0.8, beginning at T = 5.0; the pattern for the synapse on the third cylinder was unchanged. Thus, in this case, the initial activations occurred at sites nearer the soma, and were followed by bursts at more remote sites. The differences between the two patterns are striking. Curve 1 has a delayed but high peak with many oscillations between 1.1 and 1.2 mV, and then drops off sharply. Curve 2 has a faster rise and maintains a minimum potential of over 0.3 mV for almost all the time during which activations occur, sometimes having peaks of 0.7 to 0.8 mV. These results are in agreement with the results shown in Figures 8 and 9 for the order effects of single activations. Thus, initial activations in more remote regions, followed by activations nearer the soma result in higher and sharper peaks in somatic potential, while the reversed order results in lower but prolonged values of potential.

Figure 22 illustrates some further explorations of the theoretical effects of complex spatio-temporal activation patterns. All parameters in these three curves were identical to those used in computations for curve 1 of Figure 21, except for the specific modifications mentioned below. Curve 3 of Figure 22 shows a theoretical somatic potential for an activation pattern which was identical to curve 1 of Figure 21 except that the locations of two synapses were changed. The distance of the synapse on the third cylinder was changed from 2.0 to 3.0, and that of the second synapse on the second cylinder from 3.0 to 2.0. The activations at the synapses at Z = 1.0 and Z = 2.0 on the second cylinder were begun at T = 4.5 and T = 4.0 respectively, with interactivation intervals

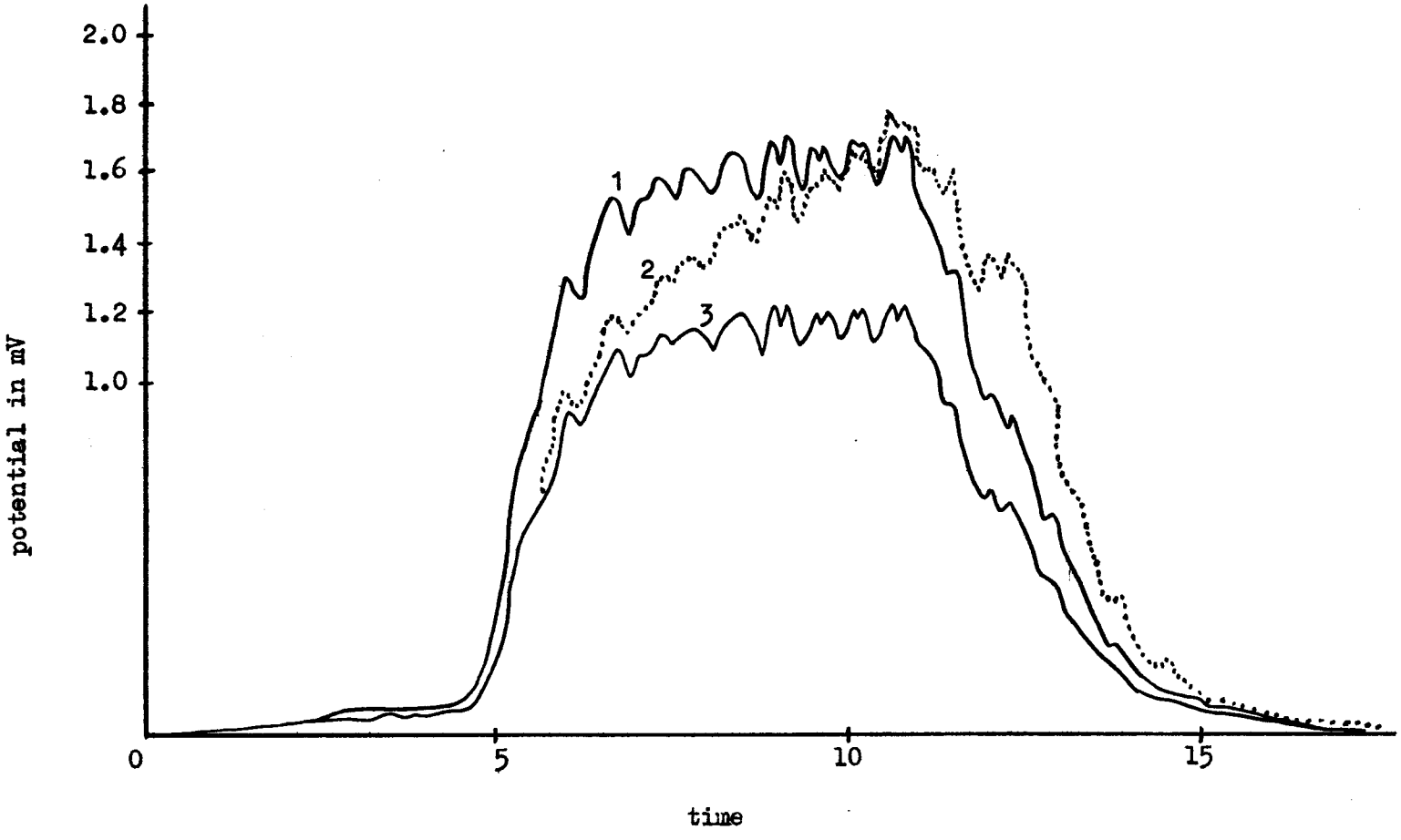

Figure 22. Comparisons of some complex activation patterns. For curve 3, q = 5 at each of five synaptic sites; curve 1 corresponds to values of q = 7 at the same synaptic sites; curve 2 shows theoretical effects of facilitation at two sites.

of 0.8. Except for slight changes in the positions and relative amplitudes of the individual peaks, the resulting theoretical somatic potential was almost identical to that of curve 1 of Figure 21. The peaks for both curves ranged from 1.1 to 1.2 mV and the overall time courses were essentially the same.

Curve 1 of Figure 22 was computed for exactly the same parameters as curve 3 of this figure, except that the value of q for all five synapses was raised from 5 to 7. Corresponding values of the peaks were increased to the same degree, some reaching values of 1.7 mV.

One of the most interesting comparisons of the study is made with reference to curves 2 and 3 of Figure 22. Curve 2 shows the theoretical somatic potential computed for the same parameters as curve 3, except that the value of q was incremented by one for successive activations at both synapses on the second cylinder, from q = 1 to q = 9. Successive increases in individual PSPs are termed "facilitation" (Katz, 1966), so curve 2 may be considered to represent facilitation at two synapses. The maximum value of curve 2, 1.772 mV, is well above all of curve 3 and is slightly above the maximum of 1.703 mV for curve 1. The effectiveness of facilitation becomes more evident when the theoretical total quantal amounts of transmitter are compared. For curve 3, with q = 5 for five sites, and 10 activations at each, a total of 250 quantal units were required to produce the theoretical curve. For curve 1, with q = 7 for all five sites, and 10 activations at each, a total of 350 quantal units were required to produce a correspondingly higher potential. However, for curve 2, with q = 5 for three sites and 10

activations at each, and q varying from 1 through 9 for the 10 activations at the other two sites, a total of only 240 quantal units produced a curve with the highest peak potential. Thus, in terms of the total amount of transmitter required to produce a given somatic potential level, facilitation would seem to be a very efficient process.

Extra peaks as a function of PSP parameters and interactivation intervals

In several of the calculations, extra peaks, in many cases of fairly large amplitude, were observed. These extra peaks are significant for two reasons. First, they were produced by a strictly deterministic model, yet many of the curves have almost random appearance with respect to the location and amplitudes of peaks. Secondly, the realization that such a multiplicity of peaks can result from an apparently simple input pattern has important consequences for the interpretation of experimentally recorded EPSP profiles. Many of the figures showing these extra peaks bear a close resemblance to experimental records. A further, and possibly quite important observation is that many of these extra peaks deviate from the expected or smooth curves by approximately the same amount as fluctuations in experimental recordings (e.g., see Eccles, 1957).

The presence, observed numbers, and amplitudes of the extra peaks depend upon the shape of the individual PSPs arriving at the soma and upon the interactivation intervals. The shape of the PSPs upon arriving at the soma in turn depends upon the quantities T_p, A, and q, and upon the distance of the synapse from the soma.

Some insight concerning the conditions which give rise to extra peaks may be gained by consideration of Figure 23. For Figure 23a, a cardboard template was moved along a baseline and its outline traced at regular intervals, as shown by the lower lines. The upper curve shows the resulting temporal summation which would occur if each of these curves moved past a point separated by such intervals. No extra peaks are observed. However, in Figure 23b, a template of a different shape was used, and again outlined at several points. The upper line shows the resulting temporal summation, and this time, some small extra peaks are seen. Figure 23c shows the same wave shapes as Figure 23b, but spaced at closer intervals, this time producing extra peaks large enough to be confused with the original peaks.

From re-examination of some of the figures in which extra peaks were observed, e.g., Figures 17, 18, and 20, it is seen that the appearance of extra peaks was delayed until after the first few activations occurred. It should also be noted that extra peaks were produced by either temporal summation of repeated activations at a single synapse, or by activations at more than one synapse, and at synapses on more than one dendritic cylinder. The important factor is how the profile of each dendritically-produced PSP looks as it arrives at the soma. The long tails of each of these component PSPs provide enough temporal summation to change the effective shape of the arriving waves, which accounts for their delay in appearance until the third or fourth activation in some cases. Thus, the appearance of extra peaks in the present deterministic model could prove useful in interpretation

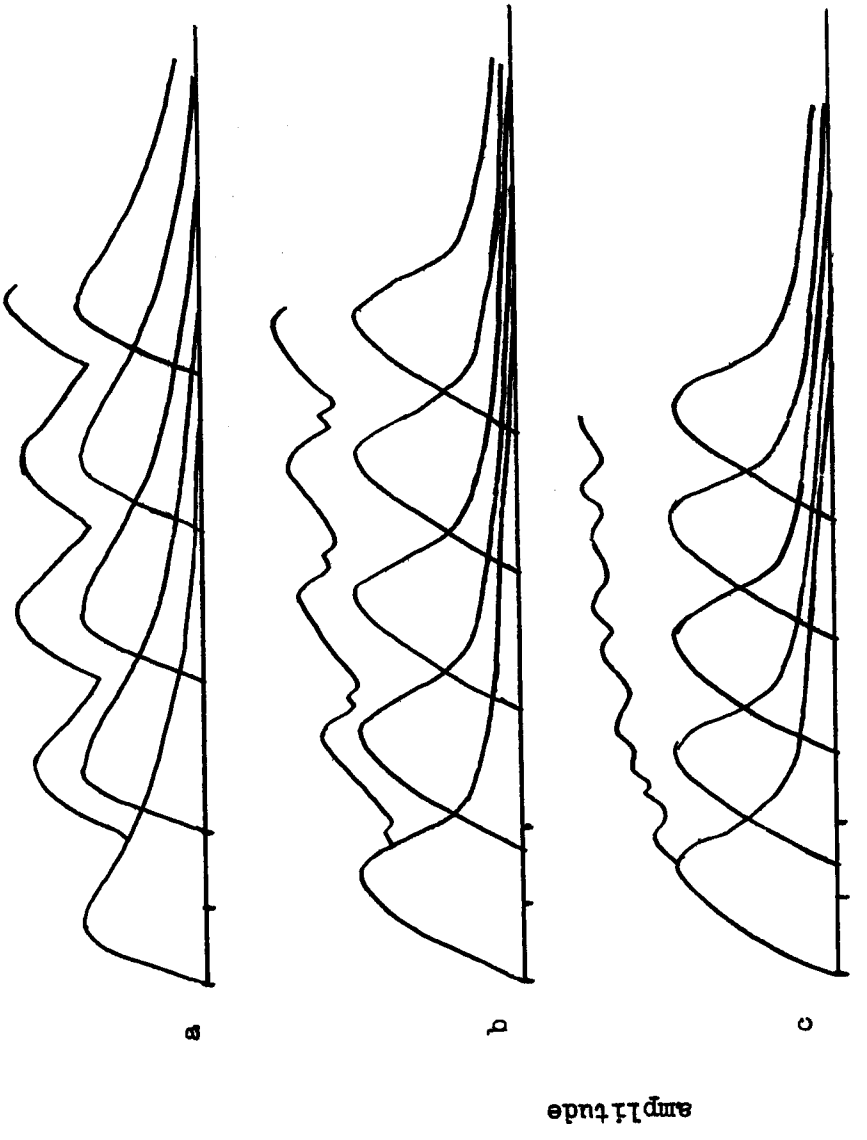

Figure 23. Appearance of extra peaks as function of wave shape and interaction interval. Relative times between activations are indicated by the 3 scale marks at the beginning of each set of curves.

of experimentally recorded PSPs, and their occurrence may be explained by spatio-temporal summation at the soma, which depends on the parameters related to the PSPs.

Experimental evidence concerning dendritic activations

Although Rall has developed a quantitative model for the role of dendritic activations in neuronal function, he was not the first to suggest the possible importance of such activations. Evidence and suggestions regarding the importance of graded responses in dendrites have accumulated rapidly in the last few years, beginning with studies by O'Leary and Bishop (1943), Bishop and Clare (1952), and Bishop (1956). These earlier studies were concerned with cortical recordings with gross electrodes. Studies with intracellular electrodes have provided further evidence of the role of dendritic activations. Brookhart and Fadiga (1960), Fadiga and Brookhart (1960), and Machne et al., (1959) recorded evoked EPSPs in frog motoneurons produced by either dorsal root or lateral column stimulation. Dorsal root stimulation typically evoked a complex multiple EPSP, while lateral column stimulation evoked a simple unitary EPSP. Further, the EPSPs produced by dorsal root stimulation showed a slow rise time, while those produced by lateral column stimulation showed a rapid rise time. On the basis of these studies, they concluded that the dorsal roots have axodendritic synapses on these motoneurons, while the lateral column fibers have axosomatic synapses on the neurons. These results are consistent with Rall's model and the present model. Further evidence concerning related studies may be found in reviews by Brookhart and Kubota (1963) and Purpura (1967).

Rall and his associates have initiated a series of theoretical and experimental studies related to Rall's models (Smith et al., 1967; Nelson and Frank, 1967; Burke, 1967; Rall, 1967; Rall et al., 1967). The first of these studies (Smith et al., 1967) was concerned with the measurement of impedance (or permeability) changes accompanying either excitatory or inhibitory PSPs in cat spinal motoneurons. The study was designed to determine whether physiologically effective synapses were located predominantly near the soma as Eccles (1964) maintains, or whether they may also be located on the dendrites as Rall's model predicts. The basis of the study was concerned with the following distinctions. If the physiologically effective synapses were located on the soma, as Eccles maintained, the action of chemical transmitter at such synapses would produce corresponding conductance changes (measured by impedance changes) which should be detected by electrodes in the cell soma, and the measured impedance change would be directly proportional to the recorded EPSP. On the other hand, if some of the effective synapses were on the dendrites as Rall predicted, then the conductance changes accompanying their activations would only occur at the synapses, and not be detected at the soma, and only the resulting EPSP at the soma would be detected, since the local potentials would propagate to the soma. The results were in support of Rall's model, with respect to the location of excitatory synapses.

Nelson and Frank (1967) found further support for Rall, in a study of the effects of hyperpolarization on PSPs. Hyperpolarizing currents decrease membrane resistance so that the resulting EPSPs

should have smaller amplitudes. Polarization applied at the soma would be expected to have a pronounced effect on EPSPs produced by synapses on the soma, while there would be little effect on EPSPs produced by dendritically located synapses. The results supported the notion of dendritic locations of some effective synapses.

Burke (1967) studied the composite nature of the monosynaptic EPSP in cat spinal motoneurons. He found that the EPSPs were composed of numerous miniature EPSPs. There were wide variations in waveform of the EPSPs. He concluded that his findings were in accord with the notion of widely scattered dendritic and somatic locations of the synapses.

Rall (1967) applied his compartmental model to interpretations of experimental data, and defined parameters of PSP wave shape which could be used to aid in inferring the distance of synapses from the soma.

Rall et al (1967) presented further applications of the shape indices defined by Rall in the preceding study, and considered possible distinctions between chemical and electrical transmission at synapses. The results were consistent with Rall's model.

Garcia Ramos (1969) studied responses of cat spinal motoneurons produced by activation over different pathways. He interpreted his results as evidence that dendritic inputs play a role in modulation of cell firing ability.

The study by Mendell and Henneman (1968) discussed in another section, also was in support of Rall's model.

Jacobson and Pollen (1968) measured distances of dendritic branch points from the soma and diameters of dendritic branches of cat

pyramidal cells. Then they used theoretical resistance calculations to predict the magnitudes of somatic potentials which could theoretically result from uniform synaptic activation in the apical dendrites at a distance of 750 μ from the soma. For depolarizations of 20 mV in these remote regions, the theoretical somatic potentials were found to be 0.4 to 0.6 mV, or about 2 to 3 percent of the dendritic potentials. The authors pointed out that even this small amount of somatic depolarization could significantly affect the firing frequency of a neuron already depolarized at a near-threshold level.

Redman and Lampard (1968) and Redman et al., (1968) stimulated cat spinal motoneurons via stochastic input frequencies over several afferent fibers, and recorded the resulting firing patterns of the motoneurons. In the former study, lower frequencies of stimulation produced less temporal summation, which is a finding consistent with the present model. A graded excitability of motoneurons in the pool was observed, which supports the study by Mendell and Henneman (1968), and in addition, the related theoretical suggestions in the section on learning and memory mechanisms in the present study. Redman et al., (1968) found that there was an optimal stimulus or input frequency in terms of the observed firing frequency of a motoneuron, i.e., beginning at lower input frequencies, the output firing frequency increased with increasing input frequency, and then decreased with further increases of input frequency. This experimental observation provides support for the theoretical results presented in this paper concerning optimal interactivation intervals, if one assumes active synapses were located

at different electrotonic distances from the soma in the above study. The investigation by Mendell and Henneman (1968) provides evidence that such synapses are located at varying distances from the soma.

In summary, the experimental evidence supports the notion that activations at dendritically located synapses can produce significant potential changes at the soma, in a manner consistent with both Rall's model and the present model. In addition, there is experimental evidence in agreement with the present model with respect to the existence of optimal input frequencies.

Consequences of some hypothetical learning and memory mechanisms upon neuronal excitability

If synaptic plasticity is a learning and memory mechanism, it must operate in such a way that use of a given synapse results in its having an increased efficacy in the future. One specific way in which this effect could be achieved is for activity at a synapse to result in synthesis of a greater amount of transmitter and for more transmitter to be released per impulse from the pre-synaptic membrane in the future. As discussed previously, the size of the PSP has been found to be directly proportional to the amount of transmitter in many types of nerve junctions (Katz, 1966; Martin, 1966). It was shown in the present study that such changes could indeed produce increased levels of somatic potential, and several such modifications could produce significant changes in somatic membrane potential, in terms of neuronal activation.

A second mechanism by which synaptic plasticity could be achieved is the growth of new synaptic endings from an axon which already has one or more functional synaptic endings on the postsynaptic neuron, so that even more endings are formed on the same neuron. A single impulse over the axon would then result in the release of transmitter from more presynaptic endings. This type of mechanism is also consistent with the experimental evidence mentioned above and with the results of the present study.

Two other hypothetical mechanisms for synaptic plasticity which have been suggested are the enlargement of extant synaptic end-bulbs or the growth of new synapses so that two neurons not previously connected become connected. In terms of the experimental evidence and of the present study, both of these mechanisms would produce the necessary increased excitability of the postsynaptic neuron, the former mechanism being subject to the restriction that the amount of available transmitter in the presynaptic ending would probably have to increase in at least the same proportion as the increase in area of the synaptic junction.

Other mechanisms, such as changes in the post-synaptic membrane which would allow the same amount of transmitter to produce a greater effect upon membrane conductance and the corresponding potential change, would also produce the elevation of somatic potential necessary for increased excitability.

It was shown that synapses which are further from the soma could become functionally as effective as those nearer the soma by increasing

the quantal amounts of transmitter released for activations at those synapses. If a synapse had its efficacy increased by one of these mechanisms, a lower input frequency occurring at that synapse in the future might be able to produce about the same level of somatic potential as a much higher frequency in the past. For example, curve 3 of Figure 14 was produced by an interactivation interval of 0.4, for five activations with Z = 1, q = 2, and a somatic potential of over 0.2 mV resulted. The effect of a sizable increase in q may be seen by comparing this curve with curve 1 of Figure 13, which was produced by a longer interactivation interval of 1.0 (and thus a lower input frequency) for five activations with Z = 1, q = 8; the resulting somatic potential had peaks as high as 0.4 mV. Thus, while very high input frequencies might be necessary to effect the change in synaptic efficacy, considerably lower input frequencies might serve to produce the same effects after the change.

Finally, one of the most important results with significant consequences for possible learning and memory mechanisms, is the observation that the precise spatio-temporal input pattern produces characteristic somatic potential variations. Alterations in a given pattern can have striking effects on the resulting somatic potentials. The timing of inputs arriving at different synapses of different neurons would seem to be a very important factor in allowing neurons to selectively respond to different spatio-temporal patterns.

Further implications for learning and memory mechanisms and for neuronal function in general may be seen from such characteristic

spatio-temporal response patterns. Mendell and Henneman (1968) investigated the distribution of terminals of single afferent fibers from spindle receptors in cat gastrocnemius muscle in the pool of approximately 300 motoneurons which innervate the muscle. They found evidence that a single afferent fiber has terminals on many motoneurons. They further stated that the wide variations in amplitude, rise time, and subsequent time courses of the observed EPSPs suggested that the numbers and locations of the synapses on the various motoneurons were consistent with Rall's model. These observations may be related to the present model. Consider a single fiber which has synaptic endings on many motoneurons at various distances from the soma. For purposes of simplification, assume that each of these endings releases the same amount of transmitter for every arriving impulse, and that the time constants for all postsynaptic neurons are identical. Now for a given temporal impulse pattern, say a fixed frequency, along a single fiber, exactly the same frequency of impulses arrives at every one of the synaptic endings of this fiber. For each synapse at a given location, the effect of this temporal pattern is to produce a characteristic local PSP pattern which in turn propagates to the soma. From the investigations in the present study, it was seen that the resulting somatic potentials vary widely in amplitude and shape for different temporal patterns of inputs occurring at synapses at different distances from the soma. The net effect of the impulse pattern from this single fiber is then to select one subset of neurons which might have sharp, high peaks in their somatic potentials, another

which might have prolonged, but smaller elevations of somatic potential, and still others of various other patterns. Now consider a second afferent fiber which also has synaptic terminals on several motoneurons in the pool, and many of these synaptic endings from the second fiber may be located on neurons which also have endings from the first fiber. A given temporal impulse pattern in the second fiber also has the end result of producing characteristic somatic potential patterns in its postsynaptic neurons. Then the concurrent activity of both presynaptic fibers can select further subsets of neurons, some having higher peaks than before, due to spatial summation of potentials in those neurons receiving inputs from both fibers. Those neurons having the highest values of somatic potential will be more likely to fire than the other neurons in the pool. For example, consider three fibers, say a, b, and c, each having synapses on several neurons in the pool. Let subsets A, B, and C denote the neurons having synapses from fibers a, b, and c, respectively. Some neurons may have synapses from two of these fibers, or even all three, so let subsets AB, AC, BC, and ABC denote these subsets. If fibers a and b are active and c is inactive, then the somatic potentials of neurons in the subsets A, B, AB, AC, BC, and ABC will be changed. The greatest elevations of somatic potential will be most likely to occur in those neurons belonging to subsets AB and ABC, since both fibers have endings on these neurons. Of course, if fiber a has many synaptic endings nearer the soma on some neurons not having synapses from fiber b, those neurons might be more likely to fire than the AB or ABC neurons having more distally located synapses, even though both fibers are active.

With respect to the above discussion, it should also be noted that different subsets of neurons having the relatively higher potentials will be selected for different input frequencies, since increasing the input frequency increases the amount of temporal summation. With respect to the above example, if fixed frequencies of impulses are arriving over fibers a, b, and c, then changing the frequency over one of the fibers could change the subset of neurons having the highest somatic potential levels. Changing the frequency over another fiber could result in a still different subset of neurons having the higher potential levels. Such changes have implications for the neurophysiological phenomenon termed "recruitment", since an increased frequency of impulses over one fiber might result in a higher firing rate for the subset of neurons which were firing previously, and in addition, the increased temporal summation in other neurons having synapses from that fiber might result in more neurons firing.

Thus the present model could prove to be of considerable value in leading to a quantitative understanding of several aspects of neuronal function and neuronal interactions.

CONCLUSION AND SUMMARY

A mathematical model of the effects of spatio-temporal miniature dendritic activation patterns on neuronal somatic potential was developed. Calculations of the theoretical somatic potentials produced by various spatio-temporal input patterns were carried out on an IBM 360/75 computer.

Several relationships between various parameters were explored. The computations indicate that there are both optimum (with respect to greatest somatic depolarization) orders of activation of several synapses at fixed sites, and optimum interactivation intervals. Experimental evidence which supports these theoretical findings was cited. Some hypothetical learning and memory mechanisms were discussed, and the theoretical electrophysiological consequences ultimately effected by such mechanisms were studied.

As is the case with any model, the present model has certain limitations. First, the limitations which Rall mentioned for the equivalent cylinder apply to the present model (see page 19), since it incorporates the equivalent cylinder model. Second, only excitatory PSPs of small amplitude were studied. Third, nonlinear summation of PSPs was not considered. Fourth, the mathematical idealization of each incoming equivalent cylinder being balanced by its identical negative counterpart is not as biologically realistic as one would like. Even with these limitations, the model can still provide some quantitative insights concerning complex activation patterns in neurons. The good agreement of the theoretical calculations with the experimental evidence

cited would seem to indicate that the limitations are not severe. Further, most of these limitations can be eliminated by refinements of the model. For example, nonlinear summation of PSPs could be included by use of approximations, and the balancing of each equivalent cylinder by its negative counterpart could possibly be eliminated by changing the boundary value problem.

In the Introduction, the question of the utility of a mathematical model was discussed, with special mention of whether a particular model would be able to show relationships which were not deducible from the experimental literature. The appearance of extra peaks in the theoretical somatic potential curves seems to provide a good example of this feature in the present model. For example, upon inspection of curves like the lower curve of Figure 18, it is not at all obvious that 20 evenly spaced activations on a single cylinder generated the curve. A given experimentally observed PSP may be generated by many possible spatio-temporal input patterns (Rall, 1967). The appearance of extra peaks in the present study adds another dimension to the interpretation of experimental recordings, with respect to the variety of possible input patterns leading to an observed somatic potential curve.

The model is useful for a variety of applications. It allows the study of any spatio-temporal input pattern, stochastic or deterministic, with variable quantal amounts of transmitter at any synaptic site. It thus allows the study of EPSP profiles as a function of various activation patterns, the theoretical calculation of EPSPs due to both facilitation and accommodation and to theoretical learning and memory

mechanisms, and with longer stimulation times, the effects of variable storage, synthesis, and release rates of transmitter at a given synapse could be studied.

LIST OF REFERENCES

Bishop, G. H. 1956. Natural history of the nerve impulse. Physiol. Rev. 36:376-399.

Bishop, G. H., and M. H. Clare. 1952. Sites of origin of electric potentials in striate cortex. J. Neurophysiol. 15:201-220.

Briggs, M. H., and G. B. Kitto. 1962. The molecular basis of memory and learning. Phychol. Rev. 69:537-541.

Brookhart, J. M., and E. Fadiga. 1960. Potential fields initiated during monosynaptic activation of frog motor neurons. J. Physiol. (Lond.). 150:633-655.

Brookhart, J. M., and K. Kubota. 1963. Studies of the integrative function of the motor neurone, pp. 38-61. In G. Moruzzi, A. Fessard, and H. H. Jasper (ed.) Progress in Brain Research. Vol. 1: Brain mechanisms. Elsevier, Amsterdam.

Burke, R. E. 1967. Composite nature of the monosynaptic excitatory postsynaptic potential. J. Neurophysiol. 30:1114-1137.

Cole, K. S. 1968. Membranes, ions and impulses. University of California Press, Berkeley.

Coombs, J. S., D. R. Curtis, and J. C. Eccles. 1956. Time courses of motoneuronal responses. Nature 178:1049-1050.

Coombs, J. S., D. R. Curtis, and J. C. Eccles. 1959. The electrical constants of the motoneurone membrane. J. Physiol. Lond. 145:505-528.

Coombs, J. S., J. C. Eccles, and P. Fatt. 1955a. The electrical properties of the motoneurone membrane. J. Physiol. Lond. 130:291-325.

Coombs, J. S., J. C. Eccles, and P. Fatt. 1955b. The inhibitory suppression of reflex discharges from motoneurones. J. Physiol. Lond. 130:296-413.

Davis, L. Jr., and R. Lorente de No. 1947. Contribution to the mathematical theory of the electrotonus. Studies from the Rockefeller Institute for Medical Research. 131:442-496.

Eccles, J. C. 1957. The physiology of nerve cells. Johns Hopkins Press, Baltimore.

Eccles, J. C. 1964. The physiology of synapses. Springer-Verlag, Berlin.

Fadiga, E., and J. M. Brookhart. 1960. Synaptic activation of different portions of the motor neuron membrane. Amer. J. Physiol. 198:693-703.

Fatt, P., and B. Katz. 1953. The effect of inhibitory nerve impulses on a crustacean muscle fibre. J. Physiol. Lond. 121:374-389.

Gaito, J. 1961. A Biochemical approach to learning and memory. Psychol. Rev. 68:288-292.

Gaito, J. 1963. DNA and RNA as memory molecules. Psychol. Rev. 70:471-480.

Gaito, J., and A. Zavala. 1964. Neurochemistry and learning. Psychol. Bull. 61:45-62.

Galambos, R. 1961. A glia-neural theory of brain function. Proc. Nat. Acad. Sci. U. S. 47:129-136.

Garcia, Ramos J. 1969. On the physiology of dendrites. Currents in Mod. Biol. 3:74-84.

Griffith, J. S., and H. R. Mahler. 1969. DNA ticketing theory of memory. Nature 223:580-582.

Grundfest, H. 1967. Synaptic and ephaptic transmission, pp. 358-372. In G. C. Quarton, T. Melnechuk, and F. O. Schmitt (ed.), The Neurosciences Rockefeller University Press, New York.

Haggar, R. A., and M. L. Barr. 1950. Quantitative data on the size of synaptic end-bulbs in the cat's spinal cord. J. Comp. Neurol. 93:17-36.

Harmon, L. D. 1964. Problems in neural modeling, pp. 9-30. In R. F. Reiss (ed.) Neural theory and modeling. Stanford University Press, Stanford, California.

Harmon, L. D., and E. R. Lewis. 1966. Neural modeling. Physiol. Rev. 46:513-591.

Hartline, D. K., and I. M. Cooke. 1969. Postsynaptic membrane response predicted from presynaptic input pattern in lobster cardiac ganglion. Science 164:1080-1082.

Hebb, D. O. 1949. Organization of behavior. Wiley, New York.

Hodgkin, A. L., and A. F. Huxley. 1952. A quantitative description of membrane current and its application to conduction and excitation in nerve. J. Physiol. 117:500-544.

Hodgkin, A. L., and W. A. H. Rushton. 1946. The electrical constants of a crustacean nerve fibre. Proc. Roy. Soc. B. 133:444-479.

Hyden, H. 1959. Biochemical changes in glial cells and nerve cells at varying activity, pp. 64-89. In Biochemistry of the central nervous system, Proc. of the Fourth Int. Cong. of Biochemistry. Vol. 3. Pergamon Press, London.

Illis, L. 1964. Spinal cord synapses in the cat. The normal appearances by the light microscope. Brain 87:543-554.

Jacobson, S., and D. A. Pollen. 1968. Electrotonic spread of dendrite potentials in feline pyramidal cells. Science. 161:1351-1353.

Katz, B. 1966. Nerve, muscle, and synapse. McGraw Hill, New York.

Katz, J. J., and W. C. Halstead. 1950. Protein organization and mental function. Comp. Psychol. Monogr. 20:1-38.

MacGregor, R. J. 1966. A Digital computer model of spike elicitation by postsynaptic potentials in single nerve cells. Rand Corporation Memorandum RM-4877-ARPA.

MacGregor, R. J. 1968. A Model for responses to activation by axodendritic synapses. Biophys. J. 8:305-318.

MacGregor, R. J. 1967. A Quantitative statement of the generator theory of nerve. Ph.D. thesis, Purdue University.

Machne, X., E. Fadiga, and J. M. Brookhart. 1959. Antidromic and synaptic activation of frog motor neurons. J. Neurophysiol. 22:483-503.

Mackie, A. G. 1965. Boundary value problems. Hafner Publishing Company, New York.

Martin, A. R. 1966. Quantal nature of synaptic transmission. Physiol. Rev. 46:51-66.

Mendell, L. M., and E. Henneman. 1968. Terminals of single Ia fibers: distribution within a pool of 300 homonymous motor neurons. Science. 160:96-98.

McCulloch, W. S., and W. Pitts. 1943. A Logical calculus of the ideas immanent in nervous activity. Bull. Math. Biophys. 5:115-133.

Nelson, P. G., and K. Frank. 1967. Anomalous rectification in cat spinal motoneurons and effect of polarizing currents on excitatory postsynaptic potential. J. Neurophysiol. 30:1097-1113.

Nelson, P. G., and H. D. Lux. 1970. Some electrical measurements of motoneuron parameters. Biophys. J. 10:55-73.

O'Leary, J. L., and G. H. Bishop. 1943. Analysis of potential sources in the optic lobe of duck and goose. J. Cell. Comp. Physiol. 22:73-87.

Plonsey, R. 1969. Bioelectric phenomena. McGraw Hill, New York.

Purpura, D. P. 1967. Comparative physiology of dendrites, pp. 372-392. In G. C. Quarton, T. Melnechuk, and F. O. Schmitt (ed.). The Neurosciences. Rockefeller University Press, New York.

Rall, W. 1959. Branching dendritic trees and motoneuron membrane resistivity. Exp. Neur. 1:491-527.

Rall, W. 1960. Membrane potential transients and membrane time constant of motoneurons. Exp. Neur. 2:503-532.

Rall, W. 1962a. Theory of physiological properties of dendrites. Ann. N. Y. Acad. Sci. 96:1071-1092.

Rall, W. 1962b. Electrophysiology of a dendritic neuron model. Biophys. J. 2:145-167.

Rall, W. 1964. Theoretical significance of dendritic trees for neuronal input-output relations, pp. 73-97. In R. F. Reiss (ed.), Neural theory and modeling. Stanford University Press, Stanford, California.

Rall, W. 1965. Dendritic synaptic patterns: experiments with a mathematical model, pp. 238-243. In D. R. Curtis and A. K. McIntyre (ed.), Studies in Physiology. Springer-Verlag, New York.

Rall, W. 1967. Distinguishing theoretical synaptic potentials computed for different soma-dendritic distributions of synaptic input. J. Neurophysiol. 30:1138-1168.

Rall, W. 1969a. Distributions of potential in cylindrical coordinates and time constants for a membrane cylinder. Biophys. J. 9:1509-1541.

Rall, W. 1969b. Time constants and electrotonic length of membrane cylinders and neurons. Biophys. J. 9:1483-1508.

Rall, W., R. E. Burke, T. G. Smith, P. G. Nelson, and K. Frank. 1967. Dendritic location of synapses and possible mechanisms for the monosynaptic EPSP in motoneurons. J. Neurophysiol. 30:1169-1193.

Redman, S. J., and D. G. Lampard. 1968. Monosynaptic stochastic stimulation of cat spinal motoneurons. I. Response of motoneurons to sustained stimulation. J. Neurophysiol. 31:485-498.

Redman, S. J., D. G. Lampard, and P. Annal. 1968. Monosynaptic stochastic stimulation of cat spinal motoneurons. II. Frequency transfer characteristics of tonically discharging motoneurons. J. Neurophysiol. 31:499-508.

Ruch, T. C., H. D. Patton, J. W. Woodbury, and A. L. Towe. 1961. Neurophysiology. W. B. Saunders Company, Philadelphia.

Sabah, N. H., and K. N. Leibovic. 1969. Subthreshold oscillatory responses of the Hodgkin-Huxley cable model for the giant squid axon. Biophys. J. 9:1206-1222.

Shilov, G. E. 1968. Generalized functions and partial differential equations. Gordon and Breach, New York.

Smith, T. G., R. B. Wuerker, and K. Frank. 1967. Membrane impedance changes during synaptic transmission in cat spinal motoneurons. J. Neurophysiol. 30:1072-1096.

Stevens, C. F. 1966. Neurophysiology: a primer. Wiley, New York.

Swigert, C. J. 1970. A Mode control model of a neuron's axon and dendrites. Kybernetik 7:31-41.

von Neumann, J. 1956. Probabilistic logics and the synthesis of reliable organisms from unreliable components, pp. 43-98. In C. E. Shannon and J. McCarthy (ed.), Automata Studies. Princeton University Press, Princeton, New Jersey.

APPENDIX A. List of symbols

The left-hand column lists the page on which a symbol first appears.

Page	Symbol	Definition
13	$V = V_m - E_r$	potential change of membrane; deviation from resting potential
13	E_ε	excitatory synaptic equilibrium potential
13	E_j	inhibitory synaptic equilibrium potential
11	C_m	membrane capacity per unit area
11	G_r	resting membrane conductance per unit area
11	G_ε	excitatory membrane conductance per unit area
11	G_j	inhibitory membrane conductance per unit area
11	$R_m = 1/G_r$	resting membrane resistance per unit area
11	$R_\varepsilon = 1/G_\varepsilon$	excitatory membrane resistance per unit area
11	$R_j = 1/G_j$	inhibitory membrane resistance per unit area
13	V_e	potential of external conducting medium
13	V_i	potential of internal medium
13	$V_m = V_i - V_e$	membrane potential
13	I_m	total current flow through membrane in radial direction
13	t	time in msec.
13	g_{Na}	sodium conductance

Page	Symbol	Definition
13	g_K	potassium conductance
14	x	distance from soma along dendritic fiber
15	τ	membrane time constant
15	R_i	specific resistance of intracellular medium
15	R_e	specific resistance of extracellular medium
15	r	radius of nerve fiber
15	λ	characteristic length
18	T	normalized time
18	X	normalized distance
18	n	number of branches of equal radius present at any distance, x, from the soma
19	s	dendritic surface area
19	Z	electrotonic distance from soma
19	K	parameter defining classes of dendritic trees
20	I_ℓ	longitudinal current in a nerve fiber
20	r_i	axoplasmic resistance per unit length
22	$E_\epsilon - V$	driving potential at excitatory synapse
29	$E_j - V$	driving potential at inhibitory synapse
21	$F(x, t)$	general notation for input forcing function
26	d	diameter of synapse

Page	Symbol	Definition
20	r_e	extracellular resistance per unit length
29	p	maximum number of equivalent cylinders
27	i	index number for equivalent cylinders
27	j	index number for synapses on a given branch or cylinder
27	m	maximum number of synapses on a branch
27	k	index number for activation times at a given synapse
27	n_j	maximum number of activation times at a given synapse
27	T_{jk}	the Kth activation time for jth synapse
27	Z_j	location of the jth synaptic site
27	q_{jk}	number of quantal releases for jth site at time T_{jk}
27	$V_j\ (T, T_{jk})$	unit PSP at jth site due to activation at time T_{jk}
27	$\delta\ (Z - Z_j)$	delta function specifying location of jth synapse
28	A	peak amplitude of input potential transient
28	T_p	time to peak in normalized time
29	$V_i\ (Z, T)$	potential at point Z on ith equivalent cylinder at time T
29	$V_s\ (T)$	somatic potential due to contributions of all equivalent cylinders

APPENDIX B. Transformation of integral

The integral expression in equation (19) has an infinite discontinuity at $T = \tau$, due to the term $\sqrt{T - \tau}$ in the denominator, so a transformation is used to allow the integral to be evaluated in the computer program. Let $U = \sqrt{T - \tau}$, so $U^2 = T - \tau$, and $2UdU = -d\tau$. Then the computational formula is

$$V(Z,T) = \sum_{j=1}^{m} \int_0^{\sqrt{T}} \frac{1}{\sqrt{\pi}} e^{-U^2 - \frac{(Z-Z_j)^2}{4U^2}} \sum_{k=1}^{n_j} q_{jk} V_j(T-U^2, T_{jk})\, dU.$$

NORTH CAROLINA STATE UNIVERSITY

INSTITUTE OF STATISTICS

(Mimeo Series available at 1¢ per page)

702. WEGMAN, EDWARD J. and D. WOODROW BENSON, JR. Estimation of the mode with an application to cardiovascular physiology. August 1970. 15

703. LEADBETTER, M. R. Elements of the general theory of random streams of events. August 1970. 21

704. DAVIS, A. W. and A. J. SCOTT. A comparison of some approximations to the k-sample Behrens-Fisher distributions. August 1970. 10

705. RAJPUT, B. S. and STAMATIS CAMBANIS. Gaussian stochastic processes and Gaussian measures. 24

706. MOESCHBERGER, MELVIN L. A parametric approach of life-testing and the theory of competing risks. August 1970. 105

707. GOULD, F. J. and JOHN W. TOLLE. Optimality conditions and constraint qualifications in Banach space. 19

708. REVO, L. T. On classifying with certain types of ordered qualitative variances: an evaluation of several procedures. 200

709. KUPPER, LAURENCE and DAVID KLEINBAUM. On testing hypotheses concerning standardized mortality rations and/or indirect adjusted rates. 13

710. SCOTT, A. J. and M. J. SIMONS. Clustering methods based on likelihood ratio criteria. 19

711. CAMBANIS, S. Bases in L_2 spaces with application to stochastic processes with orthogonal increments. 9

712. BAKER, CHARLES R. On covariance operators. September 1970. 11

713. RAJPUT, B. S. On abstract Wiener measures. 14

714. SCOTT, A. J. and M. J. SIMONS. Prediction intervals for log-linear regression. 15

715. WILLIAMS, OREN. Analysis of categorical data with more than one response variable by linear models. 112

716. KOCH, GARY and DONALD REINFURT. The analysis of complex contingency table data from general experimental designs and sample surveys. 75

717. NANGLIK, V. P. On the construction of systems and designs useful in the theory of random search. 11

718. DAVID, H. A. Ranking the players in a round-robin tournament. 20

719. JOHNSON, N. L. and J. O. KITCHEN. Tables to facilitate seeking S_B curves II. Both terminals known. 21

720. SARMA, R. S. Alternative family planning strategies for India; a simulation experiment. Thesis.

721. SUWATTEE, PRACHOOM and C. H. PROCTOR. Some estimators, variances and variance estimators for point cluster sampling of digraphs. November 1970. Thesis. 211

722. DIONNE, ALBERT and C. P. QUESENBERRY. On small sample properties of distribution and density function estimators. November 1970. Thesis. 61

723. EVANS, J. P. and F. J. GOULD. Stability and exponential penalty function technique in non-linear programming. 18

724. HARRINGTON, DERMOT. A comparison of several procedures for the analysis of the nested regression model. 132

725. QUALLS, CLIFFORD and HISAO WATANABE. An asymptotic 0-1 behaviour of Gaussian processes. 1971. 13

726. SEN, P. K. Convergence of sequences of regular functionals of Empirical distributions to processes of Brownian motion.

727. CRAMER, HARALD. Some personal recollections of the development of statistics and probability.

728. BAKER, CHARLES R. Joint measures and cross-covariance operators.

729. NEELEY, DOUGLAS LEE ROY. Disequilibria and genotypic variance in a recurrent truncation selection system for an additive genetic model. Ph.D. Thesis. 1971

730. WEGMAN, EDWARD J. and CHRIS R. KUKUK. A time series approach to the life table.

731. MOORE, GEORGE WILLIAM. A mathematical model for the construction of cladograms. Ph.D. thesis. 1971. 262

732. BEHBOODIAN, JAVAD. On the distribution of a symmetric statistics from a mixed population. 1971.

733. BEHBOODIAN, JAVAD. Bayesian estimation for the proportions in a mixture of distribution.

734. SEN, P. K. Robust statistics procedures in problems of linear regressions with specific reference to quantitative bio-assay, II.

735. CAMBANIS, STAMATIS. Representation of stochastic processes of second order and linear operations.

736. QUALLS, CLIFFORD and HISAO WATANABE. Asymptotic properties of Gaussian processes.

737. ANDERSON, R. L. and L. A. NELSON. Some problems in the estimation of single nutrient response functions. 34